



CANADA

DEPARTMENT OF MINES AND  
TECHNICAL SURVEYS, OTTAWA

MINES BRANCH  
RESEARCH REPORT

R 40

PRICE 25 CENTS

## GRAIN BOUNDARIES IN METALS

- A. GRAIN BOUNDARY MELTING
- B. FURTHER OBSERVATIONS ON  
GRAIN BOUNDARY MELTING
- C. GRAIN BOUNDARY SHEAR IN ALUMINUM

by

F. WEINBERG

PHYSICAL METALLURGY DIVISION

A.&B. REPRINTED FROM ACTA METALLURGICA  
VOL. 5, NO. 8, 1957 & VOL. 6, NO. 8, 1958

C. REPRINTED FROM TRANS. OF THE METALLURGICAL  
SOCIETY OF AIME, VOL. 212, DEC. 1958

1958

182166210

# GRAIN-BOUNDARY MELTING\*†

F. WEINBERG‡ and E. TEGHTSOONIAN§

Using bicrystal specimens of tin, the melting behavior of grain boundaries has been examined as a function of stress, heating rate, boundary angle, and impurity concentration. For small-angle boundaries (less than  $12^\circ$ ) there is no tendency for the crystals to part at the boundary during melting. However, specimens with large-angle boundaries were consistently observed to separate at the boundary during melting. The temperature at which the separation took place, over a wide range of stress and heating rates, was the same as the melting temperature of the bulk material within the experimental accuracy of  $0.02^\circ\text{C}$ . The actual separation occurred a finite interval of time after the onset of general melting, and this interval was determined as a function of test conditions.

Adding impurities to the material affected the melting temperature of the boundary in a manner conforming with that expected from their phase diagrams.

Similar tests have been conducted on aluminum bicrystals. It has been determined (within an experimental accuracy of  $0.25^\circ\text{C}$ ) that, as in the case of tin, the large-angle boundaries separated only after the melting temperature of the bulk material had been reached. Specimens of aluminum with low-angle boundaries (less than  $14^\circ$ ) were not observed to separate at the boundary.

## FUSION DES JOINTS DES GRAINS

En utilisant des échantillons bicristallins d'étain, les auteurs examinent le comportement, à la fusion, des joints en fonction des tensions, de la vitesse de chauffe, de l'angle des joints et de la concentration des impuretés. Pour des frontières à petit angle (inférieur à  $12^\circ$ ), il n'y a pas de tendance pour les cristaux à se séparer au joint pendant la fusion. Il a été observé cependant que des échantillons avec des angles forts se prêtent à une telle séparation.

Pour une large gamme de tensions et de vitesses de chauffe, la température à laquelle la séparation a lieu est la même que la température de fusion de la masse du métal dans les limites de la précision des mesures ( $0,02^\circ\text{C}$ ). Cette séparation a lieu dans un intervalle fini de temps après le début de la fusion générale et celui-ci a été déterminé en fonction des conditions expérimentales.

L'addition d'impuretés au métal, affecte la température de fusion du joint d'une manière conforme aux prévisions des diagrammes de phase.

Des essais analogues ont été effectués sur des bicristaux d'aluminium. Il a été démontré (avec une précision expérimentale de  $0,25^\circ\text{C}$ ) que, comme pour l'étain, les joints à grand angle ne se déparent que lorsque la température de fusion de la masse est atteinte. Des échantillons d'aluminium avec un angle des joints faible n'ont pas montré une séparation au joint.

## SCHMELZVORGANG AN KORNGRENZEN

An Zweikristallproben aus Zinn wurde das Verhalten der Korngrenzen beim Schmelzen in Abhängigkeit von der Spannung, der Aufheizgeschwindigkeit, dem Korngrenzwinkel und der Verunreinigungskonzentration untersucht. Bei Kleinwinkelkorngrenzen (weniger als  $12^\circ$ ) ergeben sich beim Aufschmelzen keine Anzeichen für ein Auftrennen des Kristalls entlang der Korngrenze. Im Gegensatz dazu war an Proben mit Grosswinkelkorngrenzen stets zu beobachten, dass beim Schmelzen der Zusammenhalt an der Korngrenze verlorengeht. Die Temperatur, bei der dieser Prozess stattfindet, stimmt über einen weiten Variationsbereich von Spannung und Erhitzungsgeschwindigkeit innerhalb der experimentellen Fehler von  $0,02^\circ\text{C}$  mit der Schmelztemperatur des gesamten Materials überein. Die tatsächliche Trennung an der Korngrenze erfolgte um ein endliches Zeitintervall später als der Beginn des allgemeinen Schmelzvorgangs. Dieses Zeitintervall wurde in Abhängigkeit von den Versuchsbedingungen bestimmt.

Verunreinigungszusätze beeinflussen die Schmelztemperatur der Korngrenze in gleicher Weise, wie dies das entsprechende Zustandsdiagramm erwarten lässt.

Ähnliche Versuche wurden an Zweikristallen aus Aluminium durchgeführt. Dabei wurde festgestellt, dass, wie beim Zinn, die Grosswinkelkorngrenzen sich erst nach Erreichen der Schmelztemperatur des Gesamtmaterials lösen (experimenteller Fehler  $0,25^\circ\text{C}$ ). Bei den Aluminium-Proben mit Kleinwinkelkorngrenzen (weniger als  $14^\circ$ ) wurde ein Auftrennen an den Korngrenzen nicht beobachtet.

## 1. INTRODUCTION

In the past few years considerable attention has been directed towards an understanding of the structure and properties of grain boundaries. Most of the experimental work has dealt with small-angle boundaries, and the results have been found to agree

\* Published by permission of the Deputy Minister, Department of Mines and Technical Surveys, Ottawa, Ontario, Canada.

† Received November 26, 1956.

‡ Physical Metallurgy Division, Mines Branch, Department of Mines and Technical Surveys, Ottawa, Ontario, Canada.

§ Now at Department of Metallurgical Engineering, University of British Columbia, Vancouver, B.C. Canada.

very well with a boundary structure described in terms of dislocation arrays. Large-angle grain boundaries, however, are still the subject of speculation. Dislocation arrays, similar to those used for small-angle boundaries, are not adequate in this case. Also, little experimental work has been reported for large-angle boundaries, since they have relatively few properties which can be examined directly. In an attempt to add to the knowledge of boundary behavior, the authors have undertaken an investigation of the manner in which grain boundaries melt.

The most extensive examination of grain-boundary melting was reported by Chalmers<sup>(1)</sup> in 1940. He performed a series of tests on controlled-orientation bicrystals of tin, and found that the melting temperature of the grain boundary was 0.14°C below that of the bulk material. This value was independent of heating rate, orientation, stress, and impurity traces over the range covered. From this he concluded that the melting-point depression was an intrinsic property of the grain boundary.

Since that time a number of other workers have reported on results obtained from aluminum. Chaudron, Lacombe, and Yannaquis<sup>(2)</sup> in 1948 estimated a boundary melting-point depression of 0.25°C for aluminum, by placing a plate of the material in a furnace of known gradient and observing boundaries melting ahead of the general interface. Pumphrey and Lyon<sup>(3)</sup> conducted tensile tests on short-test specimens of polycrystalline aluminum near the melting-point. They observed a sharp drop in the ultimate tensile stress at temperatures about 4°C below the bulk melting-point, accompanied by glazed intercrystalline fractured surfaces, from which they concluded that boundaries melt 4°C below the melting-point of the bulk material. Boulanger<sup>(4)</sup> reported on internal friction measurements near the melting-point of aluminum and its alloys. From his results he concluded that there was no incipient melting at the grain boundaries, any depression measured being a result of impurities or high stresses, leading to fracture.

The present investigation was initially undertaken with aluminum, using the controlled-orientation bicrystal type of specimens adopted by Chalmers for tin. The results suggested that the melting temperature of the boundary might be the same as that of the bulk material. As a result, it was decided to re-examine the boundary melting behavior of tin, since the thermometry was more reliable and the results could be directly related to those reported by Chalmers.

The bulk of the observations deal with tin. These

results are therefore reported first, followed by the results of the tests with aluminum.

## 2. EXPERIMENTAL PROCEDURE AND OBSERVATIONS

### 2.1. Procedure—Tin

Controlled orientation bicrystals of tin were grown from the melt in graphite boats, using the modified Bridgman technique adopted by Chalmers. The orientation of the crystals was such that a  $\langle 110 \rangle$  direction was parallel to the growth direction in both crystals, and the (001) plane initially horizontal. To produce a bicrystal having a given boundary angle  $\theta$ , each crystal was rotated  $\theta/2$  about the growth direction in an opposite sense to one another, resulting in a symmetrical tilt boundary of the specified angle. Orientations were determined by the Laue back-reflection technique.

The tin used was obtained from the Vulcan Detinning Co., and was of three grades:

- (1) Vulcan electrolytic: typically 99.9966% Sn with Fe as major impurity.
- (2) Vulcan extra pure: 99.999% Sn with Pb as the major impurity.
- (3) Vulcan spectrographic: 99.9999% Sn, 0.00001% Fe; 0.00001% Pb; 0.0001% total detectable foreign materials.

The first two grades were found to behave in a similar manner, and the results are grouped together. In the majority of the tests the first grade listed was used.

The bicrystals grown were 18 mm wide, 5 mm thick, and 100 mm long, with the boundary running approximately down the centre of the crystal perpendicular to the front face. Test specimens 10 mm wide were cut from the bicrystals with a fine saw, and the ends notched for gripping purposes. Tests were conducted on flame-cut and as-grown bicrystal specimens to ensure that the cutting operation was permissible in the present case. No detectable difference was observed.

In order to obtain satisfactory values for the depression of the melting-point at grain boundaries, it is necessary to obtain heating curves in which there is a constant controllable temperature-rise before melting, a rapid transition to the melting plateau, and a plateau of sufficient duration and constancy to indicate clearly the bulk melting temperature for each run. It is also necessary to determine when the boundary melts and to be sure that the temperature measured is that of the grain boundary.

The experimental arrangement adopted is shown in Fig. 1. The specimen was placed against a block

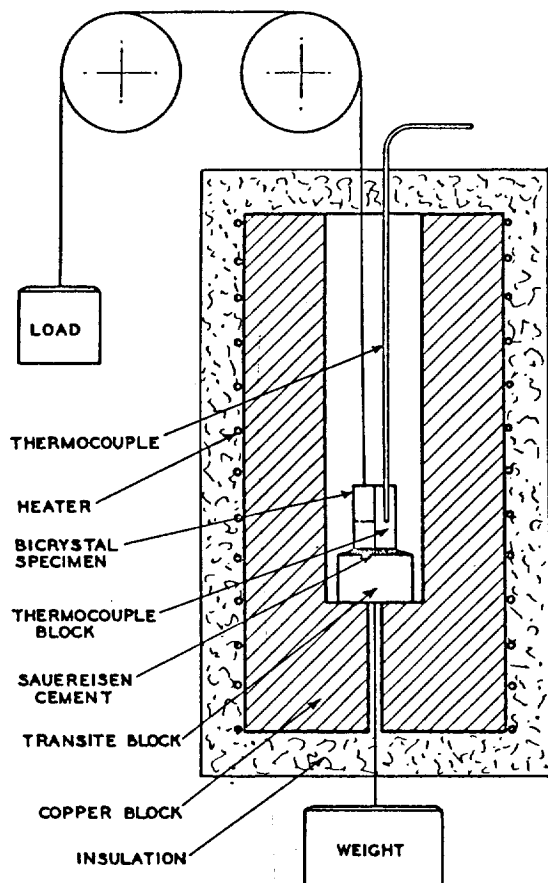


FIG. 1. Experimental arrangement for testing tin bicrystal specimens.

of similar size and material into which a chromel-alumel thermocouple had been cast. Both were placed on a transite block and fastened into position by Sauereisen cement. After the cement had hardened, the assembly was lowered into a copper block and subsequently heated. The thermocouple used was made by spot-welding 28-gage thermocouple wire. It was annealed for 1 hour at 300°C and then cast in the block with the bare junction in direct contact with the tin. The couple did not appear to contaminate or be contaminated by the tin over many runs, and thus the system was considered satisfactory. The upper half of the specimen was gripped with chromel wire wound through slots cut in the specimen. With this system, the thermal coupling between the specimen and the thermocouple block was excellent, but the coupling of the two with the copper block was poor. This enabled the heat to be distributed more uniformly throughout the specimen and the thermocouple block.

The melting curves obtained, which were considered satisfactory, had heating rates ranging from 0.25°C/min to 2.5°C/min and were constant to

within 0.02°C/min at the centre of this range. The transition from rise to plateau was completed within 15 sec and the plateau was constant within 0.02°C over a period of 10 min. The melting of the grain boundary was indicated by the falling of the weight applying the stress to the specimen. From initial tests using various sized blocks for the thermocouple, as well as second thermocouples in blocks replacing the bicrystal specimens, and from the consistency of repeated runs, it was concluded that the thermocouple in a typical test gave a true indication of the boundary temperature. Temperature measurements were made with a Leeds and Northrup  $K_2$  potentiometer, and the results believed accurate to 0.02°C.

In all of the tests the heating rate was measured and maintained constant as the specimen increased in temperature. Once the melting plateau was reached, the temperature of the specimen remained constant, whereas the copper block continued to rise at the same rate as before. The temperature difference between the specimen and copper block would progressively increase, resulting in an increased rate of heat flowing into the specimen and therefore an increased melting rate. Accordingly, although the rate of heating was constant, the rate of melting increased. The total time for a specimen and thermocouple block to melt in a typical test was approximately 30 min.

## 2.2. Observations—Tin

When a test was stopped immediately after the bicrystal had separated and the specimen subsequently examined, it was clear that separation at the boundary had taken place with little melting of the component crystals. Separation was indicated by the falling of the weight stressing the specimen. This occurred suddenly, a finite period after the specimen had reached a constant temperature. This finite delay period, to be denoted by  $t^*$ , varied from 10 to 700 sec, depending upon experimental conditions. No depression of the melting-point at the grain boundary was evident.

The behavior of the boundary was examined as a function of stress, heating rate, orientation difference, and purity. Each of these variables will be discussed in turn. The results are summarized in Table I along with those reported by Chalmers. The difference in temperature at which boundary separation occurs and the bulk melting-point is indicated by  $\Delta_{G.B.}$ .

2.21. *Stress.* A large number of tests were conducted at 100 and 2000 g/cm<sup>2</sup> and a smaller number at 50, 200, 1000, 4000, and 6000 g/cm<sup>2</sup>. In all cases the specimens separated after the plateau had been

TABLE I

Chalmers			W. & T.	
Stress (g/cm <sup>2</sup> )	1000-3000	$\frac{\Delta_{G.B.}}{0.14^{\circ}C}$	50-6000	$\frac{\Delta_{G.B.}}{0.00^{\circ}C}$
Heating rate (°C/min)	independent rate not specified	0.14°C	independent 0.1 to 3	0.00°C
Orientation difference	independent 14°-85°	0.14°C	0-11° boundary did not melt 11°-85° independent	0.00°C
Purity (%)	99.998	0.14°C	99.9999	0.00°C
	99.996	0.14°C	99.996	0.00°C
	99.986	0.14°C	+0.007% Pb → 0.1% Pb 0.1°C → 1°C	
	+0.05% Pb	0.24°C	+0.04% Sb → 0.02°C	
	+0.2% Pb	0.70°C	+0.05% Cd 0.5°C	

reached on the melting curve, indicating no depression of the melting-point within the stated accuracy of 0.02°C.

Increasing the stress decreased the length of time ( $t^*$ ) from the onset of general melting, as indicated by the melting plateau, to separation at the boundary.

In several tests the stress (100 g/cm<sup>2</sup>) was applied in shear along the boundary, instead of in tension across the boundary. The results were the same as those obtained for the tension tests.

A test was also conducted *in vacuo*, the results indicating no discernable effect due to the change in pressure around the specimen.

A visual examination was made of the surfaces exposed at the boundary, following boundary separation, in order to ascertain if there was any evidence of fracturing. It was observed that the surfaces were smooth and relatively flat for very high-purity tin (99.9999%), but consisted of a family of ridges for the less-pure material (99.996%). An example for the less-pure material is shown in Fig. 2, where the exposed surfaces of two specimens cut from adjacent sections of a parent crystal are reproduced. Specimen (a) was tested at 100 g/cm<sup>2</sup> stress, specimen (b) at 2000 g/cm<sup>2</sup>.

Ridges can clearly be seen on the exposed surfaces



FIG. 2. Exposed surfaces of two tin bicrystal specimens cut from adjacent sections of parent crystal. (a) Tested at 100 g/cm<sup>2</sup> stress, (b) 2000 g/cm<sup>2</sup> stress.

which continue from one specimen to the other with no apparent change due to the large change in stress. The ridges run in the general direction of growth of the parent bicrystal.

It is believed that the ridges are a result of the macromosaic structure usually present in crystals grown from the melt. As a result of the structure, the as-grown boundary is not plane through the specimen, but has a shape conforming with the surface shown in Fig. 2. Specimens cut from adjacent sections of a bicrystal would have similarly contoured exposed surfaces, as was observed. The very high-purity tin did not appear to have a pronounced macromosaic structure which would account for the smooth exposed surface.

These observations did not indicate any evidence of fracturing taking place on boundary separation.

A number of tests were conducted in which it was possible to watch the bicrystal surface during the test. For this the same bicrystal, thermocouple, and transite-block arrangement was used as shown in Fig. 1, but with a furnace having a window incorporated in it.

No change in appearance of the bicrystal was observed until the plateau of the melting curve was reached. At this point the boundary trace appeared on the surface and progressively widened with time. For tin of 99.9999% purity tested at 100 g/cm<sup>2</sup> the boundary widened from 0 to 0.25 mm, approximately linearly, in 160 sec. During this time shiny points appeared on the general surface, suggesting surface melting was taking place. After a period of time, depending upon test conditions, the boundary trace very suddenly increased in width an appreciable amount and flow of liquid metal could be discerned at the boundary. This was followed after a few seconds by complete boundary separation.

2.22. *Heating rate.* Over the range of heating rate examined (0.10 to 3.0°C/min) the specimens separated at the boundary after the melting plateau had been reached. Increasing the heating rate decreased  $t^*$ .

2.23. *Orientation difference.* Tests were conducted on tilt boundaries of 5°, 8°, 11°, 12°, 15°, 45°, and 80°, with electrolytic tin (99.996% Sn). These values of boundary angle are only correct to within approximately 2°, due to the lineage structure present in the specimens. Five specimens were tested at each of the two lowest angles and three at 11° at stresses ranging from 100 to 4000 g/cm<sup>2</sup>, and in all cases there was no indication of melting or separation at the grain boundaries. The tests were terminated when the specimens melted at the upper or lower support. Ten tests at 13°, five at 15°, two at 80°, and many at 45° all

clearly failed by separation at the grain boundaries.

Several tests were conducted on twist-type  $45^\circ$  boundaries, the boundary formed by rotating the seeds an equal and opposite amount about an axis perpendicular to the boundary plane. These specimens behaved similarly to the  $45^\circ$  tilt-type boundaries.

Twin boundaries were also examined to determine if they behave as large- or as small-angle boundaries. Single crystals having the  $\langle 110 \rangle$  direction parallel to the crystal axis were lightly struck in compression, resulting in a family of twins some of which extended through the specimen. These were tested in the usual way. In all cases the specimens partly recrystallized, resulting in the presence of a large-angle grain boundary which subsequently failed on heating. However, there appeared to be no melting taking place at the twin boundaries which remained in the specimen, indicating that they very likely behave as the small-angle boundaries and have no tendency for melting.

It was observed that a finite time-interval  $t^*$  elapsed from the onset of general melting, as indicated by the arrest in the heating curve, to boundary separation. This period was examined as a function of stress, orientation, and purity, and the results are reported in Fig. 3.

Curve 1 of Fig. 3 shows the variation of  $t^*$  with stress for a large-angle grain boundary of 99.996% purity. The curve is indicative of the behavior of all the large-angle boundaries tested with this purity of tin, including  $\theta = 15^\circ$ . The scatter of  $t^*$  for repeated tests was within 15 sec. Occasionally one test of an identical series resulted in a value of  $t^*$  which differed by a factor of 2 or 3 from the others for unknown reasons. These results were not used. Curve 2 shows the results for large-angle boundaries over the same stress range for higher-purity tin (99.9999%). The

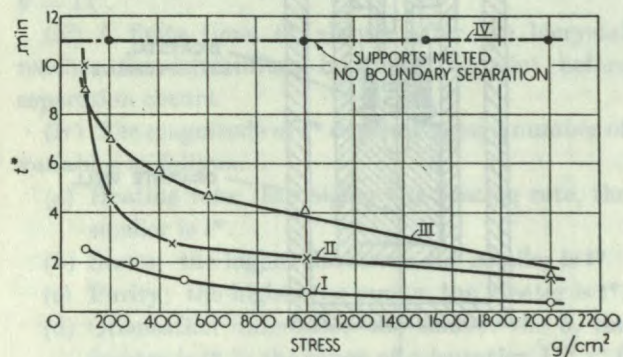


FIG. 3. Stress-dependence of time to boundary separation ( $t^*$ ) from the onset of general melting.  
 I— $45^\circ$  tilt boundary : purity 99.996%  
 II— $45^\circ$  tilt boundary : purity 99.9999%  
 III— $13^\circ$  tilt boundary : purity 99.996%  
 IV— $13^\circ$  tilt boundary : purity 99.9999%  
 Heating rate  $\frac{1}{3}^\circ\text{C}/\text{min}$ .

significant feature in this case is that at low stresses  $t^*$  increases rapidly with a decrease in stress.

The results for an intermediate angle ( $\theta = 13^\circ$ ) is shown in curves 3 and 4. For the lower-purity tin there is a further increase in  $t^*$  with decrease in stress over a larger stress range as compared with the large-angle results. For the higher-purity tin the boundary did not separate at all within the time available before the supports melted.

Small-angle boundaries (less than  $12^\circ$ ) do not separate at the boundaries, as reported earlier.

2.24. Purity. In the last section, observations were reported on the behavior of high-purity tin. This section will deal with tests on specimens having specific amounts of impurity added. The purpose of these tests was to extend the general observations of boundary separation as a function of purity, as well as to obtain further information to help ascertain if boundaries separate as a result of melting or fracturing.

If the boundaries separate as a result of melting, then it would be expected that this behavior would be directly related to the phase diagram of the materials concerned. For the case in which the solidus and liquidus temperatures drop with increased amounts of added impurity, it would be expected that the temperature of separation would drop in a corresponding fashion. On the other hand, if separation is a result of a fracturing process, then it might be expected a given amount of any impurity could lower the temperature at which separation takes place in a manner not related to the phase diagram.

Three materials were added to the electrolytic tin-lead, antimony, and cadmium, in amounts within their solid solubility range. Lead and cadmium both have solidus and liquidus temperatures which drop with increasing concentration, whereas the antimony curves rise with concentration. The results are shown in Table 2.  $\Delta_{G.B.}$  is the difference in temperature between boundary separation, and the bulk melting-point of

TABLE 2

Added impurity	wt. %	Stress $\text{g}/\text{cm}^2$	$\Delta_{G.B.}$ ( $^\circ\text{C}$ )	$\Delta_{G.B.}$ Solidus ( $^\circ\text{C}$ )
Lead	0.007	2000	0.10	0.15
	0.02	100	0.20	0.45
	0.02	2000	0.40	
	0.43	100	0.20	0.90
	0.43	1000	0.40	
	0.43	2000	0.65	
	0.43	4000	0.75	
	0.10	1000	0.90	2.10
Antimony	0.10	2000	1.10	
	0.040	2000	-0.02	-0.05
Cadmium	0.053	2000	0.70	0.70

the pure material, taking temperature-lowering as positive.

$\Delta_{G.B. \text{ solidus}}$  is the calculated depression on the solidus obtained from the phase diagram. The thermocouples used were believed to be accurate and reproducible to within  $0.05^\circ\text{C}$  on the basis of a number of tests on pure tin with the same thermocouples. The block in which the thermocouple was cast was always the same composition as the bicrystal.

The lead and cadmium alloy crystals all separated at their grain boundaries at temperatures below the melting temperature of the pure material and above the solidus temperature, completely in accord with their phase diagrams. Increasing the applied stress moved the temperature of separation closer to the solidus. With the antimony alloy crystals, the boundary separated at a temperature above the pure tin melting temperature, again in agreement with the phase diagram. The fact that the value of  $\Delta_{G.B.}$  is below the calculated solidus value is not considered significant, since this is within the reproducibility of the thermocouple used.

In considering the observations in which the lead-alloy specimens failed at the boundary below the melting-point of the pure material and the antimony above, it appeared possible that this might be explained by a fracture process. The relatively large lead atoms might weaken the boundary leading to early fracture, whereas the antimony atoms, being of similar size to that of tin, would not. If this were so, then adding cadmium to the pure material should not lower the boundary separation temperature, since cadmium and tin also have similar atomic sizes. This was not the case, suggesting that fracture is not the dominant mechanism.

### 2.3. Procedure—Aluminum

Controlled-orientation bicrystal specimens of aluminum were prepared in a manner similar to that described for tin, except in this case an argon atmosphere was used. The material was superpure French aluminum (99.995% Al). The  $\langle 100 \rangle$  direction was parallel to the growth direction in both crystals of the bicrystal, and a  $\{100\}$  plane rotated about this direction from the horizontal for each crystal, producing a symmetrical tilt boundary. Test specimens were cut from the bicrystals with a fine saw, to the shape shown in Fig. 4(a). The boundary at the centre of the test specimen was 8 mm wide, 5 mm thick, and perpendicular to the specimen face.

Temperatures were measured with a platinum resistance thermometer, using the thermal system shown in Fig. 5. Two specimens were tested at the

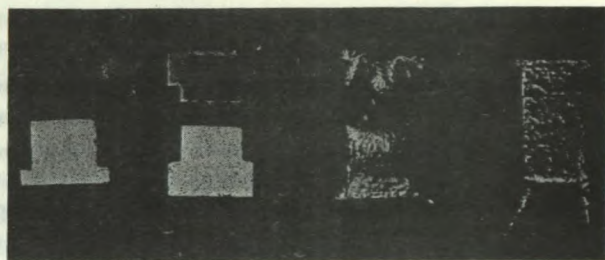


FIG. 4. Aluminum bicrystal specimens (a) before testing, (b) after testing (large angle), (c) similar to (b) but allowed to continue melting, (d) after testing (small angle).

same time, held in small graphite plates. The assembly shown was lowered into a large furnace and slowly heated. It was expected that the aluminum annulus would start to melt before the centre of the system had reached the melting-point. As a result, the graphite well and test specimens would slowly and uniformly be brought to the melting-point, enabling the thermocouple temperature to be taken as indicative of the specimen temperatures.

About sixty specimens were tested in this fashion, and it appeared that it was impossible to correlate specimen temperatures to thermometer temperature

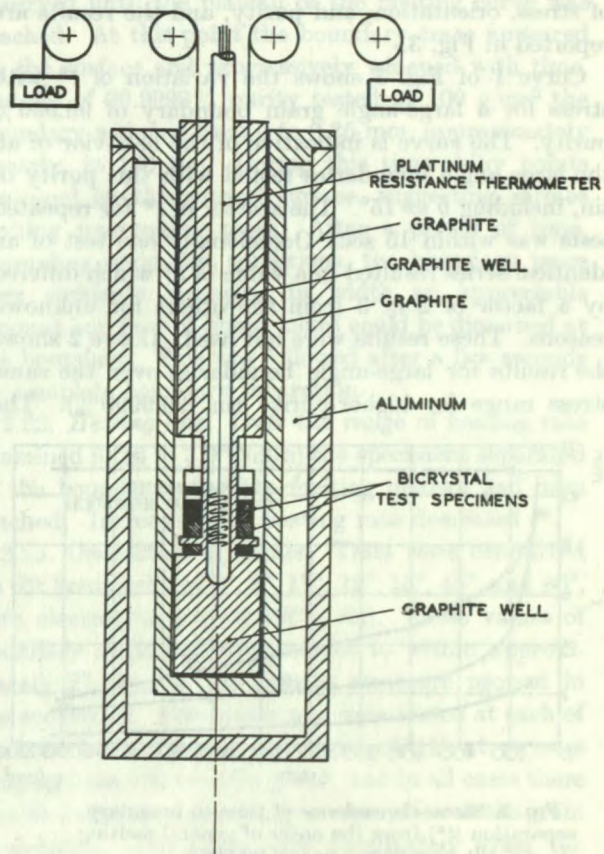


FIG. 5. Experimental arrangement for testing aluminum bicrystal specimens.

to better than 0.25°C for this system. The platinum resistance thermometer had been initially calibrated at the bulk melting-point of the material used.

#### 2.4. Observations—Aluminum

As with tin, it was observed that separation took place at the grain boundaries with little melting of the component crystals. This is shown in Fig. 4, in which a typical bicrystal specimen is shown before testing (a) and after testing under a stress of 100 g/cm<sup>2</sup> (b). If the test had been continued and appreciable melting allowed to take place, then the individual crystals would appear as shown in (c). Boundary separation took place at the bulk melting-point of the pure material within a range of 0.25°C, the possible error estimated in relating the thermometer reading to the specimen temperature.

It was observed that boundary separation only took place for large-angle grain boundaries. For small-angle tilt boundaries (less than 14°) the specimens behaved as single crystals showing no tendency toward separation. Specimen (d) of Fig. 4 is a bicrystal having a 9° tilt boundary, treated in the same manner as (c). Appreciable general melting has taken place and the specimen has failed by melting at the supporting legs with no indication of melting at the boundary.

### 3. DISCUSSION

A brief summary is given below of the observations that require explanation.

(i) Bicrystals of tin separate at the grain boundaries when heated to their melting-point. The temperature at which separation occurs is the same as the equilibrium melting temperature of tin within the experimental accuracy of 0.02°C.

(ii) This grain-boundary separation is only apparent for bicrystals with boundary angles greater than  $\theta = 11^\circ$ .

(iii) A finite time,  $t^*$ , elapses after the bicrystal reaches the equilibrium bulk melting-point before separation occurs.

(iv) The magnitude of  $t^*$  depends upon a number of variables as follows:

- (a) Heating rate; the higher the heating rate, the smaller is  $t^*$ .
- (b) Stress; the higher the stress, the smaller is  $t^*$ .
- (c) Purity; the higher the purity, the greater is  $t^*$ .
- (d) Orientation difference; the smaller the  $\theta$ , the greater is  $t^*$  in the range of orientation  $11^\circ < \theta < 15^\circ$ .

Each of the points in the summary will be discussed in turn.

(i) The fact that bicrystals separate at the boundary under stress immediately poses the question as to

whether the separation is a result of a true melting or a mechanical fracturing process. It is felt that the nature of the present results clearly indicates that it is, in fact, a melting process which is being observed in these experiments. If, as Chalmers found, the separation at the boundary took place at a temperature below the bulk melting-point, this conclusion might be somewhat doubtful. However, inasmuch as the present results clearly show that the boundary separation occurs at the bulk melting-point, and moreover at some considerable time after the onset of general melting, it is very likely that the boundary separation is due to melting at the boundary, and not due to mechanical fracturing at the boundary.

Further evidence to support this suggestion comes from the results of experiments on the bicrystals with added impurity. As described in an earlier section, all these experiments showed that the boundary separation occurred at a temperature between the solidus and liquidus temperatures (i.e. after the onset of general melting), and at a temperature that was lower than the bulk melting-point of pure tin for both lead and cadmium impurity and higher for the antimony impurity. This is in complete conformity with a true melting process that would be expected from the form of the equilibrium diagrams for these additions to tin.

In addition, the stress independence of the visual appearance of the exposed boundary surfaces confirms a true melting process rather than a boundary-fracture process.

(ii) Perhaps the most striking item in the summary is the relatively straightforward observation that for boundary angles less than 11° there is no tendency for boundary separation to occur whatsoever, while for boundary angles greater than 11° this tendency is inevitably present to a degree controlled by other variables. These observations suggest that either one or both of two things change markedly at this critical angle; these are (1) the geometrical structure of the grain boundary and (2) the composition in the grain-boundary region. The first of these two changes is in general agreement with the model of grain-boundary structures proposed by Read and Shockley<sup>(5)</sup> in their discussion of grain-boundary energies. Considering, in the simplest case, that a low-angle boundary is constituted of an array of edge dislocations, it follows that the density of dislocations increases with boundary angle until, at about  $\theta = 12^\circ$ , the dislocations are separated by a distance of about four atom spacings. This is about the distance at which one might expect the beginning of serious overlap of the dislocation cores resulting in the loss of identity of



the individual dislocations. For small angles, the grain-boundary region would be relatively orderly, for large angles relatively disorderly. At intermediate angles, where the dislocations overlap and lose their identity, there would be a general increase in the disorder of the boundary region, the disorder becoming more or less continuous throughout the region. It is probably significant that the critical angle of about  $11^\circ$  observed in the present work coincides quite closely to the  $\theta_m = 12^\circ$  of the Read and Shockley energy equation for tin.

The second possibility to be considered is the change in composition in the grain-boundary region that occurs with change in boundary angle. As suggested by the work of Thomas and Chalmers<sup>(6)</sup> on bicrystals of lead containing bismuth impurity, the character of the grain-boundary segregation of the impurity is orientation sensitive, being very low for small angles (up to about  $15^\circ$ ) and then increasing very rapidly for increasing boundary angle. Even though Thomas and Chalmers also observed a marked decrease in grain-boundary segregation with increasing temperature, it is still very possible that when the boundary angle is satisfactory for grain-boundary segregation to occur, that such segregation is likely to persist to some degree right up to the melting-point.

From the present observations it does not appear possible to separate the effect of atomic disorder and the effect of the presence of foreign atoms at the boundary on the boundary melting behaviour. The fact that below a critical boundary angle the boundary does not melt, and that this angle coincides with the critical angle from boundary-energy calculations, suggests that the dominant factor is the boundary structure. However, if one assumes that boundary melting is a result of the presence of impurities, and the impurity concentration at the boundary is directly related to the boundary structure, then the same observations could be satisfactorily explained.

That impurity atoms do play a major role in the boundary behavior is suggested by the results obtained with a boundary angle ( $\theta = 13^\circ$ ) close to the critical value. Increasing the purity of the tin from 99.996% to 99.9999% was sufficient to change the basic observation. With the lower-purity material the specimens all separated at the boundary over the full stress range used; with the higher-purity tin there was no separation. These results also suggest that only a very small concentration of impurity would be required at the boundary to effect separation. The influence of this concentration on the melting temperature would be much smaller than that detectable by the present thermal system, accounting for the

observation that separation takes place at the same temperature as the equilibrium bulk melting temperature.

(iii) To explain why a finite time-interval  $t^*$  elapses from the onset of general melting to boundary separation, and why this interval varies the way it does with experimental conditions, requires a discussion of the detailed melting process at the boundary. Since melting along the boundary was not directly observed, the mechanism must be inferred from the boundary behavior.

Consider first the behavior of a single crystal suspended in the centre of a furnace as it is slowly heated. Melting would first start on the outside surfaces of the specimen, since heat is flowing from the outside to the centre of the specimen and melting can nucleate more readily on a surface than in the centre of a crystal. Melting would then proceed progressively toward the centre of the specimen, as shown schematically in Fig. 6(a), where the lines show successive positions of the melting fronts. The rate of melting would be a function of the rate of heat-input into the crystal.

Next consider the behavior of a bicrystal containing a large-angle grain boundary. As with a single crystal, melting would start on the outside surface, but the shape of the melting front would be influenced by the presence of the boundary. It is believed that a large-angle boundary consists of a relatively disordered region of atoms, roughly four lattice spacings wide in which, in this case, there is a concentration of impurity atoms. The boundary properties appear to be independent of the orientation of the crystals as long as the boundary angle is greater than the critical value. Under these conditions it appears reasonable to consider the boundary as consisting of two internal crystal surfaces separated by a relatively disordered region of atoms. These internal surfaces, in a similar manner to the outside surfaces, would then show a

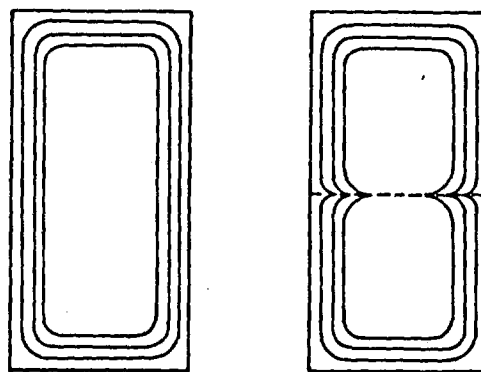


FIG. 6. Schematic diagram showing the successive positions of the melting interface for single and bicrystal test specimens.

stronger tendency towards melting than the body of the crystal. Since heat is flowing from the outside to the centre of the specimen, the outside edges of the internal surfaces would start to melt and then proceed toward the centre. The melting fronts in the case of the bicrystal would then be somewhat as shown schematically in Fig. 6(b). Grain-boundary melting would then really result from the melting of each of the members of the bicrystal on its internal surface producing a liquid layer which could not longer support the applied stress, or weight of the lower half of the specimen. The time  $t^*$  to boundary separation from the onset of general melting is the time required for the internal surfaces at the boundary to melt to the centre of the specimen producing a complete liquid layer.

(iv) (a) Consideration can now be directed to understanding the variation of  $t^*$  with variation in experimental conditions. The most readily understood is the reduction in  $t^*$  with an increase in the heating rate, for an increase in heating rate merely results in an increase in the rate of supplying the latent heat for melting and, consequently, an increase in the rate of advance of the melting front described above. This will result in a shorter time for the advancing melting fronts along the grain-boundary surfaces to meet and join into a continuous liquid layer.

(b) The sensitivity of  $t^*$  to stress may be understood by considering the relationship between melting-point and pressure. From a thermodynamic argument, following Chalmers,<sup>(1)</sup> a stress of 100 g/cm<sup>2</sup> applied to a tin specimen would produce a lowering of the melting-point of 0.001°C. It is reasonable to expect that the lowering of the melting-point due to stress would be enhanced at a grain boundary, considering the disorder at the boundary. Accordingly, once melting starts and the melting front advances into the specimen as described previously, that portion of the melting front advancing into the grain-boundary region will proceed more rapidly under the action of a stress than in its absence. Therefore, the higher the applied stress, and the more pronounced the lowering of the melting-point in the grain-boundary region, the smaller will be the time for complete melting at the grain boundary to occur. It should be emphasized that for the range of stresses used, the maximum reduction in melting-point is still less than 0.01°C.

(c) Consider the dependence of  $t^*$  on purity. Recall that tin of 99.9999% purity had a greater  $t^*$  than tin of 99.996% purity. As mentioned earlier, it is considered possible for segregation of impurity in the grain-boundary region to persist up to the melting-point. Moreover, as Cahn<sup>(7)</sup> has pointed out, the

concentration of impurities at the grain boundary at a temperature greater than the condensation temperature, is proportional to the bulk concentration. Thus it is to be expected that the concentration of impurity at the grain boundary will be greater in the 99.996% tin than in the tin of 99.9999% purity. It follows then that the melting-point of the material in the grain-boundary region will be lowered by the concentration of impurity, provided that the equilibrium diagram is of this type. Therefore the melting front will advance more rapidly along the grain boundary in a manner directly analogous to that just described for the action of stress, and the time to separation will be correspondingly reduced.

The behavior of tin specimens in which the added impurity is antimony, is somewhat anomalous. Increasing the concentration of antimony raises the melting temperature of the alloy, which should therefore decrease the tendency for melting at the grain boundary and therefore boundary separation. This was not what was observed, the specimens always separating cleanly at the boundary. The results in this case therefore suggest that, in the case of antimony in tin, the grain boundary is a region which is depleted in impurity. This is a conclusion which has not been corroborated by any other evidence.

(d) As in the case of the lowering of the melting-point in the grain-boundary region due to the applied stress, so too the difference in grain-boundary segregation concentration will likely be sufficiently small so that the lowering of the melting-point due to these segregations will again be of the order of 0.01°C. Since the experimental arrangement was such that the heating plateaus were not better than about 0.02°C, such variations were never directly observed. For bicrystals with  $\theta$  in the range of 11°–16°,  $t^*$  decreases as  $\theta$  increases and this is probably a result of the increasing amount of segregated impurities at the grain boundary in a manner similar to the orientation dependence found by Thomas and Chalmers.<sup>(6)</sup>

#### 4. CONCLUSIONS

1. Preferential melting occurs at grain boundaries.
2. This preferential melting occurs at a temperature equal to the equilibrium bulk melting temperature for "pure" tin.
3. The melting occurs only for grain-boundary angles greater than 11° and is independent of boundary angle in the range 15° to 90°, with the exception of twin boundaries.
4. The rate at which the boundary melting takes place depends upon (1) the applied stress, (2) the heating rate, (3) the purity of the material, (4) the

orientation difference in the range  $11^\circ$  to  $15^\circ$ .

5. The boundary melting phenomenon is not only an intrinsic property of the boundary itself, arising solely from the disorder in the boundary region, but is also largely controlled by trace amounts of impurity.

#### ACKNOWLEDGMENTS

The authors wish to thank Dr. R. L. Cunningham for his continued interest and support during the course of this investigation and Dr. F. W. Boswell for helpful discussions.

#### REFERENCES

1. B. CHALMERS *Proc. Roy. Soc.* **A175**, 100 (1940).
2. G. CHAUDRON, P. LACOMBE, and N. YANNAQUIS *C. R. Acad. Sci., Paris* **226**, 1372 (1948).
3. W. I. PUMPHREY and J. V. LYON *J. Inst. Metals* **82**, 33 (1953).
4. C. BOULANGER *Revue Métal* **51**, 210 (1954).
5. W. T. READ, JR. and W. SHOCKLEY *Imperfections in Nearly Perfect Crystals* p. 352. John Wiley (1952).
6. W. R. THOMAS and B. CHALMERS *Acta Met.* **3**, 17 (1955).
7. R. W. CAHN *Impurities and Imperfections* p. 47. American Society of Metals (1955).

## FURTHER OBSERVATIONS ON GRAIN BOUNDARY MELTING\*

F. WEINBERG†

The melting behaviour of grain boundaries in bicrystals of aluminum and zinc has been examined. The melting temperature of the boundary was found to be the same as that of the bulk material within an experimental uncertainty of 0.05°C for aluminum and 0.02°C for zinc. Bicrystals of zinc separated at the boundary before appreciable melting of the component crystals for boundary angles between 26° and 108°. They did not separate for angles between 0°–26° and 108°–180°. This suggests that a certain degree of order exists in some grain boundaries up to boundary angles of 72°. It also shows that boundary melting and possibly boundary energy, is significantly affected by the position of the boundary.

### OBSERVATIONS COMPLEMENTAIRES DE LA FUSION DES JOINTS DE GRAINS

L'auteur a examiné le comportement à la fusion des joints de bicristaux d'aluminium et de zinc. La température de fusion du joint est la même que celle de la matière dans son ensemble; l'erreur expérimentale est de 0,05°C pour l'aluminium et de 0,02°C pour le zinc. Les bicristaux de zinc se sont séparés au joint avant toute fusion appréciable des deux cristaux lorsque l'angle du joint est compris entre 26° et 108°. Cet effet n'apparaît pas pour les autres orientations. Il semble donc qu'un certain degré d'ordre existe à certains joints pour des angles pouvant atteindre 72°. En outre, il apparaît que la fusion du joint et probablement l'énergie du joint, est affectée sensiblement par la position du joint.

### WEITERE BEOBACHTUNGEN ZUM SCHMELZEN VON KORNGRENZEN

In Bikristallen aus Aluminium und Zink wurde das Verhalten der Korngrenzen beim Schmelzen untersucht. Die Schmelztemperatur der Korngrenze stimmt innerhalb der experimentellen Unsicherheit von 0,05°C für Aluminium und 0,02°C für Zink mit der des Kristallinneren überein. Bikristalle aus Zink trennten sich bei Korngrenzenwinkeln zwischen 26° und 108° längs der Korngrenze, bevor die einzelnen Kristalle merkbar zu schmelzen anfangen. Sie trennten sich nicht bei Winkeln zwischen 0°–26° und 108°–180°. Der Befund weist darauf hin, dass in einigen Korngrenzen ein gewisser Ordnungsgrad bis zu Korngrenzenwinkeln von 72° vorhanden ist. Er zeigt auch, daß das Schmelzen der Korngrenze und möglicherweise die Korngrenzenenergie stark von der Lage der Korngrenze abhängt.

## 1. INTRODUCTION

In a recent paper, Weinberg and Teghtsoonian<sup>(1)</sup> reported on the melting behaviour of grain boundaries in tin and aluminum. They found that boundaries melted at the same temperature as the bulk material within an experimental accuracy of 0.02°C for tin and 0.25°C for aluminum. They also observed that the tendency of the boundary to melt before appreciable melting of the component crystals depended on the boundary angle. Large angle boundaries melted readily whereas small angle boundaries showed no tendency for early melting. The critical angle between large and small angle behaviour for tin was at  $\theta = 12^\circ$  which agreed with the  $\theta_m$  of the Read and Shockley energy equation for this material. The critical value for aluminum was  $\theta = 14^\circ$ . The reasons for considering the boundary separation to be a result of

melting at the grain boundary, and not of fracture, are discussed in the earlier report.

The present report deals with the melting behaviour of grain boundaries in aluminum and zinc. Further temperature measurements have been made on aluminum bicrystals in order to reduce the reported experimental uncertainty of 0.25°C. Both the temperature of boundary melting, and the dependence of early boundary melting on boundary angle, have been examined in zinc in order to determine the boundary behaviour in a metal having a hexagonal structure.

## 2. EXPERIMENTAL PROCEDURE AND OBSERVATIONS

### 2.1 Aluminum

Controlled orientation bicrystal specimens of super-pure aluminum were used, similar in shape and orientation to the specimens described.<sup>(1)</sup> The thermal system used is shown in Fig. 1, temperatures being measured with a Meyers platinum resistance thermometer. Two bicrystal specimens were placed on opposite sides of the thermometer adjacent to the

\* Received December 2, 1957; revised version February 3, 1958. Published by permission of the Director, Mines Branch, Department of Mines and Technical Surveys, Ottawa, Ontario, Canada.

† Physical Metallurgy Division, Mines Branch, Department of Mines and Technical Surveys, Ottawa, Ontario, Canada.

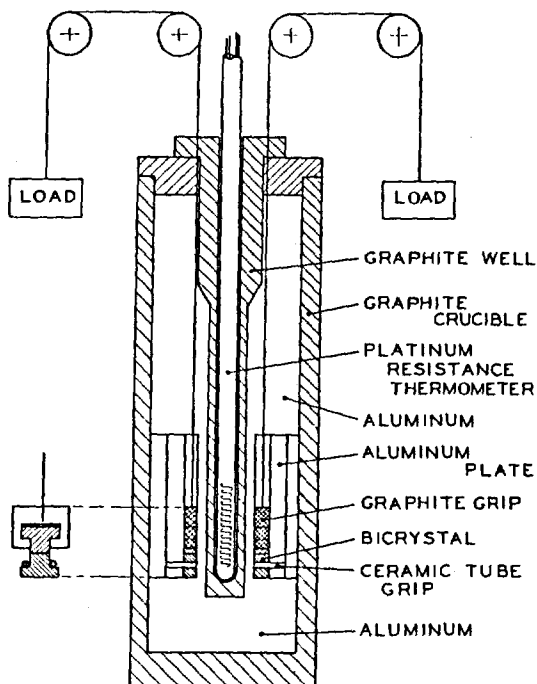


FIG. 1. Experimental arrangement for testing aluminum bicrystals.

sensitive element, each pressed against a flat surface milled on the aluminum block. In this way the temperature of the specimen could be taken as that of the block, measured by the resistance thermometer.

A series of melting curves was obtained before the aluminum block was milled, in order to calibrate the thermometer and determine the best operating conditions for the furnace. The final melting curves which were considered adequate had an initial heating rate of  $1.7^{\circ}\text{C}/\text{min}$ , a transition period of approximately five minutes, and a melting plateau which showed a temperature rise of  $0.05^{\circ}\text{C}$  over a period of twenty minutes. It was noted that milling the flat faces on the aluminum block did not change the position or shape of the melting curve.

With the bicrystal specimens in position, under a stress of  $200\text{ g}/\text{cm}^2$ , the system was heated at the rate of  $1.7^{\circ}\text{C}/\text{min}$  until the weights loading the specimens fell, following which power to the furnace was turned off. Since there was relatively little melting of the aluminum block in this time, the specimens could be examined to be sure that they had separated at the boundary.

It was observed that the bicrystals separated at their grain boundaries from two to five minutes after the onset of general melting. The measured temperature at which they separated, for a series of tests, was within  $0.05^{\circ}\text{C}$  of the value determined by extrapolating the plateau of the calibration curves to the point at

which the boundaries separated. From this it can be concluded that the boundary melting temperature is the same as that of the bulk material within an experimental uncertainty of  $0.05^{\circ}\text{C}$ .

## 2.2 Zinc

Bicrystal specimens of high-purity zinc (99.999 per cent) were prepared and tested in a manner similar to that described for tin.<sup>(1)</sup> The orientation of the component crystals was arranged such that the basal plane was parallel to the growth direction in each crystal with a  $[11\bar{2}0]$  axis also approximately parallel to the growth direction. To form a bicrystal of boundary angle  $\theta$  each component crystal was rotated through an angle  $\theta/2$  about the growth direction, in opposing senses, starting with the basal plane parallel to the boundary plane. This produced a symmetrical tilt boundary of the specified angle. Boundary angles were determined to an accuracy of  $2^{\circ}$  by cleaving the component crystals and measuring the angle formed by the cleaved planes. The values obtained were checked in several cases using back-reflection X-ray techniques.

The specimens were carefully cut from the as-grown bicrystal with a jeweller's saw, heavily etched, annealed, and then tested. In some cases acid-cut specimens were used to ensure that the cutting operation did not affect the boundary behaviour. The testing apparatus used for tin<sup>(1)</sup> was modified slightly for zinc, in that a glass sleeve was put in the furnace to prevent any contamination of the zinc by copper. A load of 50 g was used resulting in a stress of  $200\text{ g}/\text{cm}^2$  on the boundary.

The melting curves obtained for zinc were similar to those obtained for tin. With a heating rate of  $1.3^{\circ}\text{C}/\text{min}$ , the transition to the melting plateau took place within 15 sec and the plateau was constant to within  $0.02^{\circ}\text{C}$  over a period of 10 min. In all cases bicrystals having a suitable boundary angle separated cleanly at the boundary on the melting plateau. The melting temperature of grain boundaries in zinc is therefore the same as that of the bulk material within an experimental uncertainty of  $0.02^{\circ}\text{C}$ .

It was found with zinc, as with tin and aluminum, that the tendency for grain boundaries to melt before appreciable melting of the component crystals is dependent on boundary angle. The dependence is shown in Fig. 2 where the percentage of the number of specimens which separated at the boundary on melting is plotted as a function of boundary angle. At least four specimens were tested at each of the points indicated on the curve. From the curve it is seen that boundaries do not melt for  $\theta = 0^{\circ}$  to  $28^{\circ}$ , melt over the range of approximately  $26^{\circ}$  to  $108^{\circ}$ , then

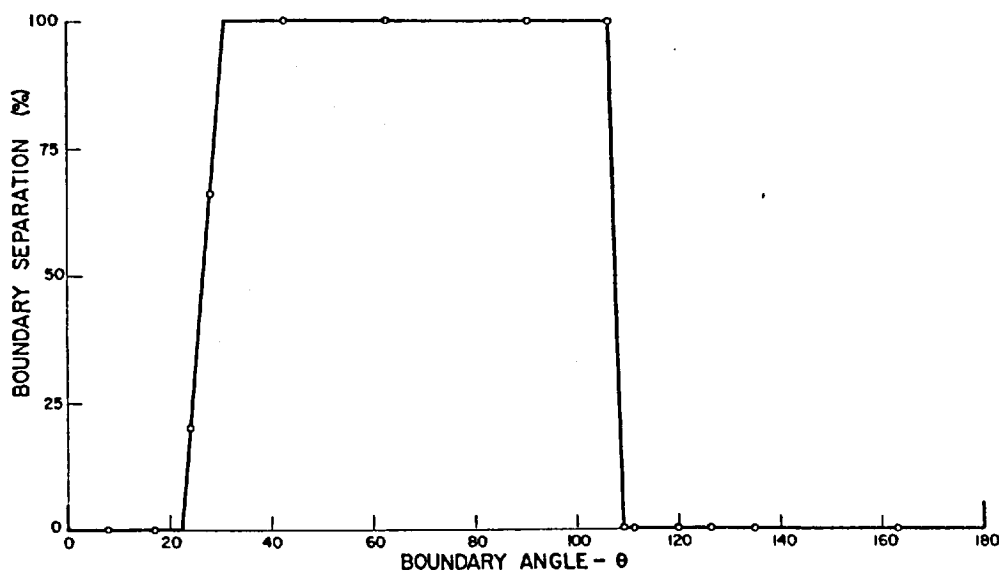


FIG. 2. The percentage of the number of specimens which failed at the grain boundary on melting, as a function of boundary angle.

do not melt for  $\theta = 108^\circ$  to  $180^\circ$ . Also, the transition from no boundary melting to boundary melting takes place over a relatively small range of boundary angle.

### 3. DISCUSSION

If one assumes that boundary melting behaviour is related to structure or lack of structure in the boundary, then there are two interesting features to be noted in the results reported in Fig. 2. First, no boundary melting occurs over the range of  $\theta = 108^\circ$  to  $180^\circ$ , an interval of  $72^\circ$ . Secondly, boundaries of angle  $\theta$  behave quite differently from boundaries of angle  $(180^\circ - \theta)$  even though the orientation difference of the two crystals forming each boundary is the same. This is illustrated in Fig. 3, in which a bicrystal consisting of crystals A and B is shown containing two boundaries, one of angle  $\theta$  and the other of  $(180^\circ - \theta)$ . It should be noted that the lattice of crystal A coincides with that of B for both  $\theta = 0^\circ$  and  $\theta = 180^\circ$ . In the results shown in Fig. 2 the reference angle  $\theta_0$  was arbitrarily taken at  $\theta = 0^\circ$ . It could equally well have been taken at  $\theta = 180^\circ$ , that is, starting with the basal planes perpendicular to the grain boundary instead of parallel to it.

The boundary melting transition at  $\theta = 26^\circ$  is what might normally be expected, since this is approximately the angle above which boundary energies in lead and silicon iron were found to be independent of boundary angle. Below  $26^\circ$  the boundary could be considered as an array of dislocations, whilst above this value the boundary would be irregular, possibly "islands of fit in a sea of misfit" as postulated by Mott.

On the basis of this argument, however, it is very difficult to account for a transition angle of  $72^\circ$  (starting at  $\theta_0 = 180^\circ$ ) since this would require dislocations to be placed about a lattice spacing apart. In this particular case the basal planes are nearly perpendicular to the boundary. It therefore seemed possible that the latter might actually consist of a number of small angle boundaries, roughly analogous to the boundary arrays in zinc single crystals bent around an axis in the basal plane and polygonized. The melting behaviour of the boundary as a whole would then depend on the largest boundary angle present. This possibility was investigated by taking back-reflection X-ray photographs of the boundary trace with a fine X-ray beam from a micro-focus unit. Within the resolving power of the technique used, the boundary was clearly observed to be single, without any small angle boundaries present. Since boundaries do not melt until a boundary angle of  $72^\circ$  is reached ( $\theta_0 = 180^\circ$ ), it appears that there

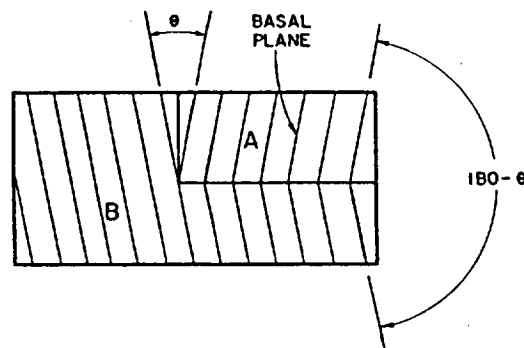


FIG. 3. A bicrystal containing two grain boundaries of boundary angle  $\theta$  and  $(180^\circ - \theta)$  respectively.

must be some atomic order in the boundary up to this value which cannot be described in terms of a simple dislocation array.

The observation that boundaries of angle  $\theta$  behave differently from those having an angle  $(180^\circ - \theta)$  shows that the boundary behaviour is a function of the orientation of the boundary in the bicrystal. This has been recognized theoretically in calculations of boundary energy and is described by Read.<sup>(2)</sup> The effect of boundary orientation is usually considered sufficiently small to be neglected, except in special cases such as twin boundaries. In the present case, only the two orientations of the boundary shown in Fig. 3 were considered; (a) when the angle between the boundary plane and the basal plane of one of the component crystals was  $\theta/2$  and (b) when this angle for the same basal plane was  $(\theta/2) + 90$ . In the range  $26^\circ < \theta < 72^\circ$ , boundaries of orientation (a) melted whereas those of orientation (b) did not.

Since the boundary melting behaviour in zinc is a function of boundary orientation, it appears that the boundary energy might also be appreciably influenced by this orientation. This follows from the observations with tin, in which the boundary melting transition angle  $\theta$  agreed with the  $\theta_m$  determined from boundary energy measurements. Measurements are being made of the relative boundary energies in zinc to ascertain if this is correct.

#### ACKNOWLEDGMENT

I should like to thank Miss L. Ng-Yelim for assistance with the measurements.

#### REFERENCES

1. F. WEINBERG and E. TEGHTSOONIAN, *Acta Met.* **5**, 455 (1957).
2. W. T. READ, JR., *Dislocations in Crystals* p. 173. McGraw-Hill, New York (1953).

# Grain Boundary Shear in Aluminum

*Observations have been made of the behavior of grain boundaries under a constant shear stress, using controlled orientation tricrystal specimens of aluminum. Grain boundary shear was observed to take place, without overall deformation of the component crystals, accompanied by localized deformation and boundary migration.*

*Measurements were made of the boundary shear as a function of time during the tests and the effects of stress, temperature, boundary angle, and added impurities were determined. From these data, curves were obtained for the stress required to produce a given shear in a given time, and it was found that this stress increased markedly when the test temperature dropped below 425°C. Attempts were made to determine an activation energy for the shear process relating shear rate with temperature, but no single activation energy was found which fitted the data.*

*Boundary shear behavior was found to depend on boundary angle. Small angle boundaries (less than 5 deg) did not shear. Large angle boundaries sheared an amount depending on both the type of boundary and size of angle. Adding small amounts of copper, iron, and silicon to the pure aluminum did not affect the shear behavior. With larger amounts of Fe (0.1 pct), no shear was observed.*

## F. Weinberg

IT has been suggested, for some time, that the behavior of metals under high-temperature creep conditions is strongly influenced by the behavior of the grain boundaries present in the material. This has led to a number of investigations<sup>1-6</sup> in which attempts were made to measure the properties of the grain boundaries themselves, both to determine their contribution to the creep process and to obtain further knowledge of their intrinsic structure and properties. The present investigation was undertaken to extend the observed data under more closely controlled experimental conditions and to attempt to clarify some of the discrepancies in the literature. A brief report of the preliminary results has been published.

### EXPERIMENTAL PROCEDURE

For the present investigation, controlled orientation specimens were used having plane boundaries which terminated at the specimen surface. Tricrystal specimens were used instead of the bicrystal type of Puttick and King,<sup>1</sup> in order to simplify the gripping technique required to apply a shear stress

along the boundary. The aluminum used was obtained from the Aluminum Francaise and was of 99.994 pct purity, containing 0.002 pct each of Cu, Fe, and Si.

The aluminum tricrystals were grown horizontally from the melt, in graphite boats, and in an argon atmosphere, following the technique developed by Chalmers.<sup>8</sup> The orientation of the tricrystals was controlled by using seed crystals separated by mica inserts. Thermal conditions were adjusted to produce tricrystals having boundaries which were macroscopically straight, parallel to the growth direction, and perpendicular to the top surface.

Following growth, the tricrystals were carefully cut with a jeweller's saw to the test specimen shapes shown in Fig. 1(a) and 1(b). In Fig. 1(a), the boundaries subjected to shear stresses are indicated AB and CD. Points A and C are the ends of the mica inserts separating the seed crystals; points B and D are at lateral cuts made in the specimen. It was found that the slots left by the mica inserts at A and C had to be enlarged slightly, by cutting, to ensure that the boundary terminated freely at these points. A shear stress was applied to the boundaries by gripping the upper two legs in file-faced Inconel grips and suspending a weight from the lower part of the specimen held in similar grips, as shown schematically in the diagram. The test specimens shown in Fig. 1(b) were cut from long

F. WEINBERG, Junior Member AIME, is Scientific Officer, Physical Metallurgy Division, Mines Branch, Department of Mines and Technical Surveys, Ottawa, Ontario, Can. Published by permission of the Director, Mines Branch, Department of Mines and Technical Surveys, Ottawa, Ontario, Can.

Manuscript submitted February 10, 1958.



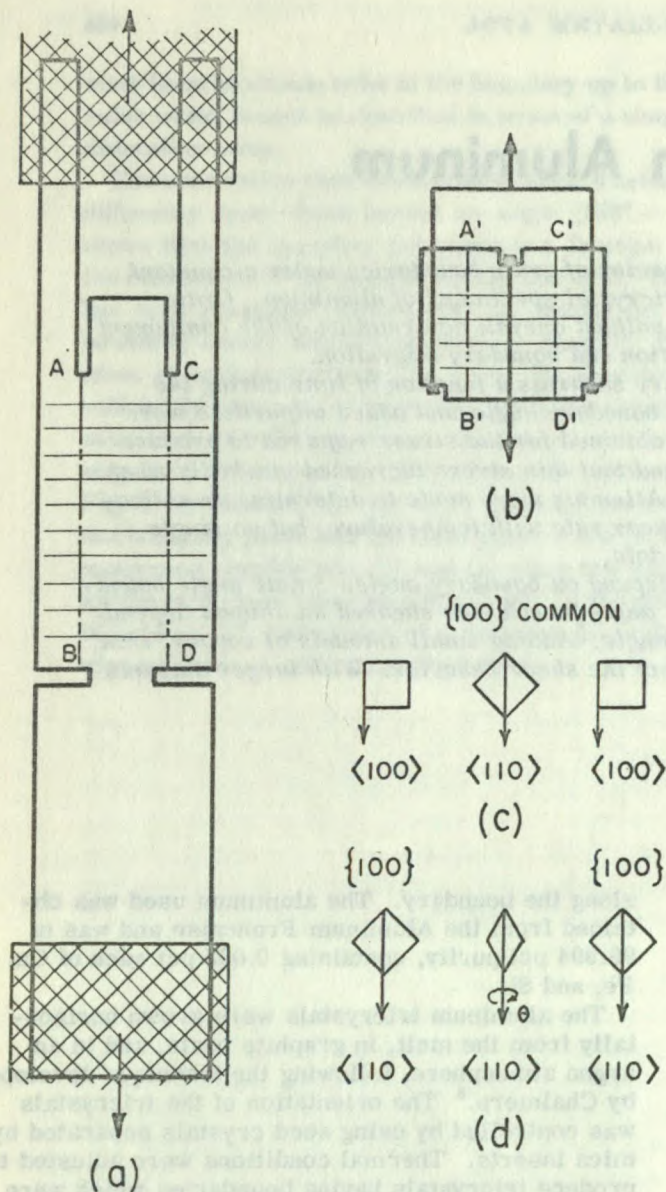


Fig. 1—(a) and (b): Diagrams of tricrystal test specimens used. The boundaries under stress are at AB and CD. (c) and (d): Orientations of the component crystals in the tricrystals.

tricrystals. They were held in Nichrome ribbon stirrups for testing, as shown schematically in the diagram.

The overall size of the specimens of Fig. 1(a) was 10 cm long, 1.8 cm wide, and 0.5 cm thick, with an effective boundary length of 3 cm for each boundary. Specimen (b) was 1.5 cm long, with the same width and thickness as (a). After cutting, the specimens were mechanically polished followed by a heavy electropolish in an ethyl alcohol perchloric acid bath. A series of fine lines were scribed on both the front and back faces of the specimen with a scratch microhardness tester. The lines were perpendicular to the boundary traces and were spaced at 2.5-mm intervals for specimen 1(a) and 2.0 mm for 1(b).

The orientation of the components of the tricrystal used in the tests is shown in Fig. 1(c) and 1(d).

Most of the boundary shear measurements, which were made as a function of time, were done with the orientation 1(c), while the effect of boundary angle on shear was done principally with 1(d). This will be referred to more fully in the observations.

The specimens were tested in split tubular creep furnaces. Their temperature was measured with chromel-alumel thermocouples tied to both ends of the specimen for type 1(a), or placed immediately adjacent to the specimen face for type 1(b). Temperature gradients in the specimen as well as fluctuations during a test were maintained within  $1.5^\circ\text{C}$  of the stated test temperature.

The position of the scratches on the specimen surface was measured during the test by looking at the surface through long double glass windows incorporated in the furnace, and making measurements along one boundary trace with a Gaertner microscope slide cathetometer. The accuracy of the measurements was a function of both the quality of the scratches and the appearance of the surface. Both of these varied during a test, the surface oxidizing, and the scratches becoming irregular in the boundary region. In the earlier part of the tests, boundary shear values—the difference between two scratch positions—were estimated to be accurate to within  $2\ \mu$ , increasing to  $5\ \mu$  as the test progressed. During the first hour of a test only the shear at the center scratch was measured, since the specimen was generally shearing rapidly. Subsequent to this, all the scratches along the boundary trace were measured and the average shear determined as well as the uniformity of the shear. Measurements of the scratch positions were also made in some cases before and after the test, in order to determine the extent of the deformation of the component crystals. After each test was completed, measurements were made of the average shear of each of the four boundary traces present on the specimen.

## OBSERVATIONS

Grain boundary shear was observed to take place when specimens were tested under suitable conditions of stress and temperature. An example is shown in Fig. 2, a type (b) specimen of Fig. 1. The boundary traces are marked AB and CD and the reference scratches are the horizontal lines spaced at 2-mm intervals. The reverse side of the specimen is similar to the side shown.

It can clearly be seen that boundary shear has taken place along the boundaries in the specimen with little overall deformation of the component crystals. This is shown by the uniform, relatively sharp break in the fiducial scratches as they cross the boundary traces, with no observable slip-line markings, bending, or movement of the reference scratches in the component crystals.

General Observations of Boundary Behavior—It was observed that boundary shear was accompanied by local deformation and boundary migration in a region immediately adjacent to the boundary. This took place for all specimens, to a greater or lesser degree, if the test was continued for a sufficient

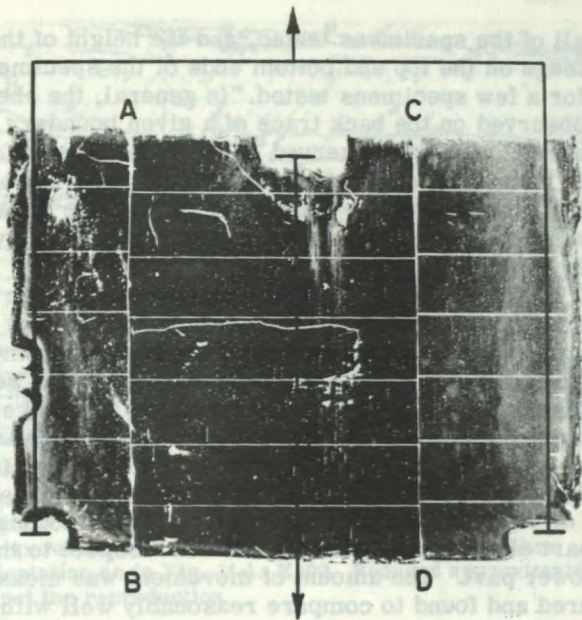


Fig. 2—Specimen of type 1(b) showing boundary shear along boundaries AB and CD. Tested at 600°C for 180 min under a shear stress of 500 g per sq cm.

length of time. The extent of the migration, slip, and distortions varied from specimen to specimen, as well as along a single boundary.

The appearance of a boundary trace at several stages during a test is shown in Fig. 3. In this particular case, the test was interrupted and the specimens cooled in order to take the photographs; however, the boundary behavior shown is generally

typical of that observed in the furnace for tests that were not interrupted. Before the stress was applied the boundary traces were not visible and the reference scratches were horizontal, continuous straight lines. It is not clear why the boundary traces appear on the surface during the test. It is likely due to a thermal etching process at the boundary, or to irregular oxidation after shear had disturbed the oxide layer.

The first two photographs of Fig. 3, taken at 15 and 60 min from the start of the test, illustrate the initial behavior of the boundary under a shear stress. After the load was applied, the boundary trace emerged as a fine vertical line accompanied by relatively sharp breaks in the reference scratches along the trace. The boundary trace then became wider and darker, the breaks in the scratches lengthened, and a group of fine lines appeared starting at the boundary and inclined to it. Some of these lines increased in length with time. The third photograph in Fig. 3, taken at 120 min from the start of the test, shows a considerable change in the appearance of the boundary region. The reference scratch has been broken into a number of segments, the boundary has apparently migrated, and a second family of fine lines has appeared, inclined to the boundary trace, between the initial and final trace positions. The rate at which the boundary moved from the initial to the final position was not determined, nor was the rate of formation of the new family of lines. The remaining photographs of Fig. 3 show the boundary trace as the test continued, showing further alternate slip and boundary migration with the formation of more

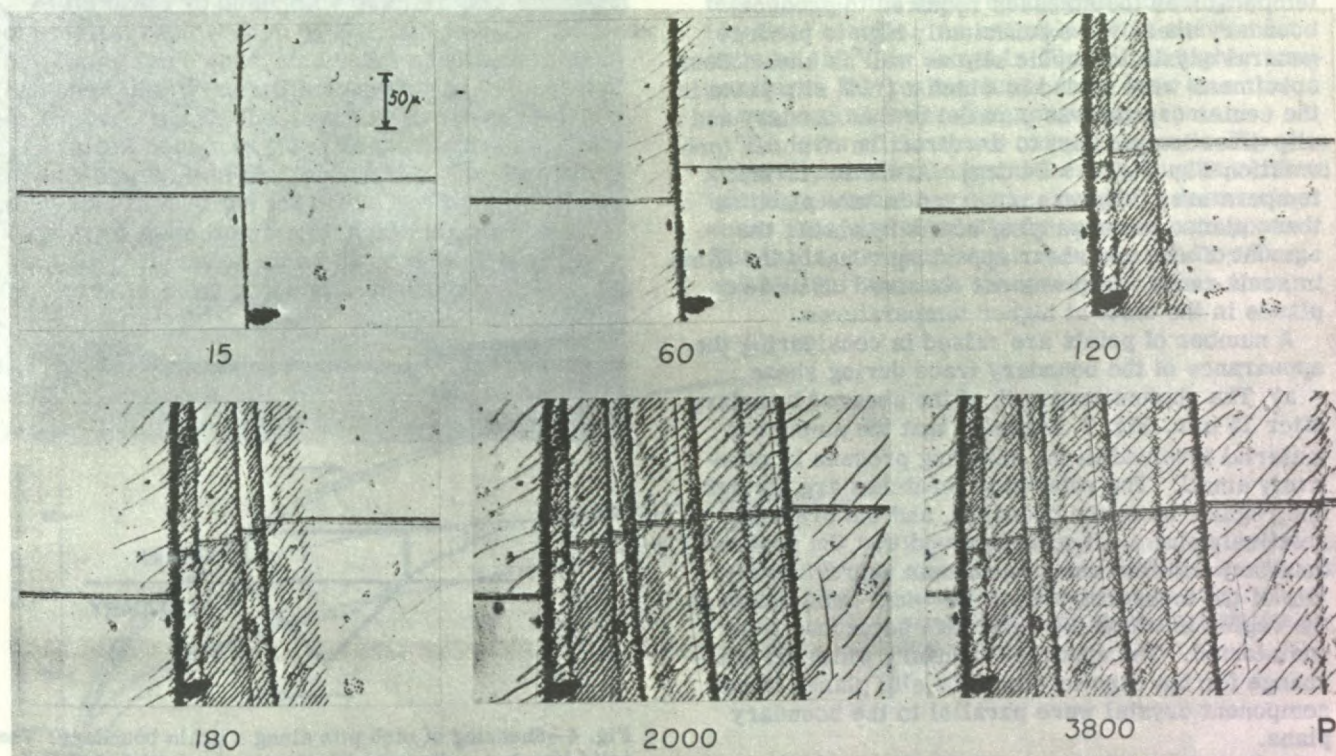


Fig. 3—Appearance of boundary trace during shear at the times indicated (min) from the application of the load. Tested at 600°C at a shear stress of 300 g per sq cm. Specimen orientation as in Fig. 1(e). X100. Reduced approximately 55 pct for reproduction.

lines on the surface as the boundary moved. After the photographs at 3800 min were taken, the specimen surface was anodized and the boundary was clearly observed to be at point P in the photograph, where shear would probably have continued to take place had the test continued.

There are several points to be noted. From the photographs it is clear that once a boundary has swept through a particular region of the specimen, that region no longer takes part in the shearing process since no further slip lines or changes appear in this area. The structure shown in the region swept out by the boundary is a record of a progressive sequence of events centered around the boundary at any given instant, and is not due to simultaneous deformation of the full region between the initial and final boundary traces.

The direction in which the boundary migrated was not constant for equivalent boundaries; in some cases, part of the boundary would migrate in one direction while the remainder would migrate in the reverse direction. In the majority of cases the center crystal grew at the expense of the outside crystals for the orientations shown in Fig. 1(c). Once the boundary did start to migrate, however, the direction of migration remained the same for the remainder of the test.

Along with the effects noted in Fig. 3, it was also observed that the surface of the region swept out by the boundary was often rumpled, regular undulations occurring every few millimeters.

At lower test temperatures there tended to be less boundary migration and more local plastic deformation adjacent to the boundary. Also, at lower temperatures the stresses required to produce boundary shear were sufficiently high to produce general crystallographic slip as well as shear. Some specimens were tested in which a  $\{111\}$  slip plane in the center crystal was parallel to the boundary and a slip direction parallel to the direction of shear (orientation Fig. 1(d)  $\theta = 54$  deg). At the lower test temperatures, slip was observed to take place on these planes accompanying boundary shear, the amount of slip and shear appearing roughly the same in some cases. Slip was not observed on these planes in the tests at higher temperatures.

A number of points are raised in considering the appearance of the boundary trace during shear.

a) The photomicrograph of the sheared boundary after 15 min, Fig. 3, suggests that the amount of material involved in the shearing process is relatively small. The reference scratches are straight and regular up to the boundary, and the break is relatively sharp. It was observed that the apparent boundary width in some cases was approximately  $\frac{1}{100}$  of the measured shear, the width being taken as the region in which the reference scratches were undistorted. The apparent boundary width did not change for the case in which the slip planes in one component crystal were parallel to the boundary plane.

b) In order to determine if the shear observed on the surface was indicative of the boundary as a whole, measurements were made of the shear on the back of the specimen as well as the front for

all of the specimens tested, and the height of the ledge on the top and bottom ends of the specimen for a few specimens tested. In general, the shear observed on the back trace of a given boundary agreed with that observed on the front face which, in turn, agreed with the step heights observed at the specimen ends. This suggests that the shears measured were indicative of the boundary behavior as a whole.

c) It is possible that strains associated with the scratches ruled on the specimen surface might result in errors in the boundary shear measurements. To check this possibility, several specimens were tested using etch pits at the boundary as markers as well as the usual reference scratches. The appearance of the etch pits after shear is shown in Fig. 4 with a sketch of the initial etch-pit shape.

It is clear, from the photograph, that the upper part of the etch pit has moved with respect to the lower part. The amount of movement was measured and found to compare reasonably well with the shear measurements made on the reference scratches of the same boundary trace. The appearance of the etch pits shown in Fig. 4 was characteristic of a number examined after shear. It is not clear why a reasonably good ledge formed only on one side of the pits.

d) Families of fine lines, as shown in Fig. 3, appeared in the boundary region when boundary shear took place. The length and regularity of the lines suggested that they might be associated with slip

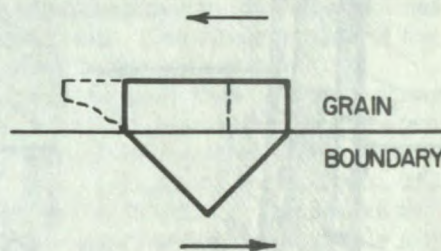
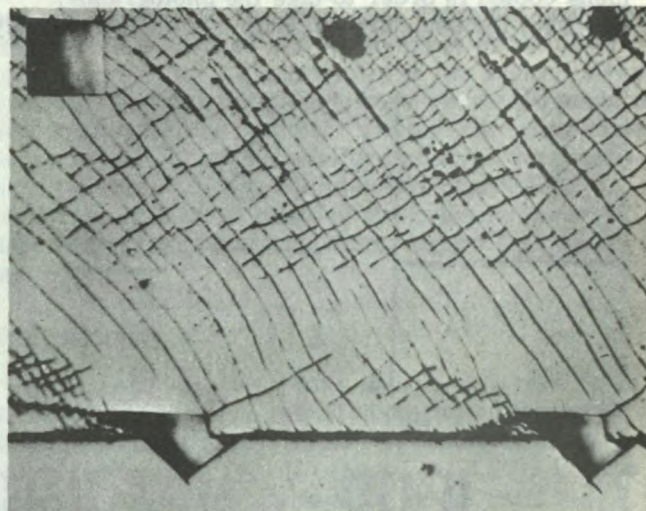


Fig. 4—Shearing of etch pits along a grain boundary. The solid line in the diagram illustrates the initial shape of the etch pit, the dotted line, the change after shear. Temperature 550° C, shear stress 500 g per sq cm. Orientation as in Fig. 1(c). X800. Reduced approximately 27 pct for reproduction.

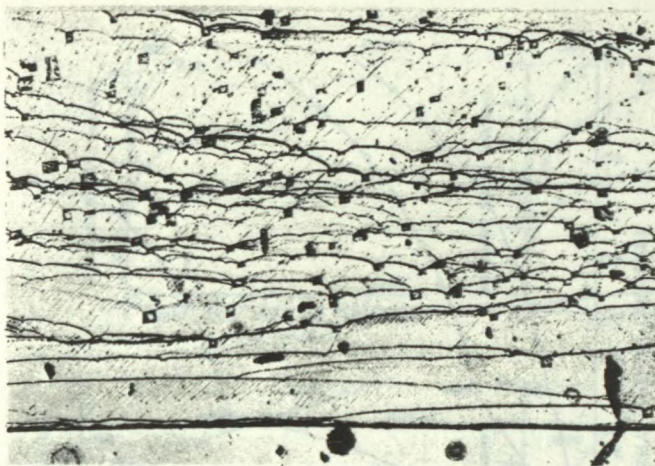


Fig. 5—Etch pits on specimen surface restraining boundary migration. Migration from bottom to top of photograph. Temperature 550°C, shear stress of 550 g per sq cm. Orientation as in Fig. 1(c). X300. Reduced approximately 28 pct for reproduction

lines resulting from the shearing process. If a slip line formed at the surface, it would likely result in a crack in the oxide layer. The position of the crack would generally correspond to the position of the slip line since the oxide is considered to be strongly adherent to the aluminum.

Attempts were made to establish whether the lines could be associated with slip lines by using multiple-beam interferometry to determine if there was a vertical step on the surface across a line. Steps were clearly observed across a few of the lines, but generally the results were inconclusive.

e) In order to determine qualitatively the effect of small irregularities on the mobility of the boundary, tests were conducted using specimens which had been lightly etched before testing. The effect of the etch pits on the boundary is shown in Fig. 5. The initial boundary trace is the horizontal line near the bottom of the photograph; the boundary migrated toward the top of the photograph. It can clearly be seen that the etch pits hindered the boundary migration since there is a cusp at the boundary at most of the pits encountered, even the

smallest. One larger etch pit, which is not shown, completely blocked the boundary from further migration. Since the boundary is seriously impeded by small irregularities in its path, this could account for the irregular shape of the boundary trace after migration and also suggests that the driving force causing the migration is small.

f) A number of specimens were anodized after testing, and the boundary regions were examined under polarized light to determine whether cells had formed as a result of the shearing process. There was no indication of cells in the boundary region, other than at a few isolated points ahead of the boundary where there had been excessive boundary migration and surface rumpling. Normal back-reflection X-ray photographs of the boundary region did not indicate any substructure, except for the lineage structure resulting from crystal growth.

**Boundary Shear—Time Measurements—Measurements of boundary shear were made at all of the scratch positions along one boundary trace during a test, and the average shear was determined. For type (a) specimens of Fig. 1 it was found that the upper legs tended to deform into the tricrystal past point A, increasing the apparent shear in this region. In this case only the measurements at the center of the boundary trace were used where there was no overall deformation of the component crystals. Below 300°C there was some deformation of the component crystals, along with the boundary shear. The deformation was primarily coarse slip resulting from the large stresses required to produce shear.**

It was found that apparently similar specimens, tested under the same conditions did not give identical results. An example of the scatter for tests at 450°C is shown in Fig. 6. At higher temperatures the scatter tends to be less than that shown, and at lower temperatures, greater.

The form of the shear curves shown in Fig. 6 is generally similar to normal creep curves, with an initial instantaneous shear, a rapidly decreasing shear rate, and a relatively constant rate portion. The initial constant shear rate reported by Tung and Maddin<sup>2</sup> was not observed, nor was a linear

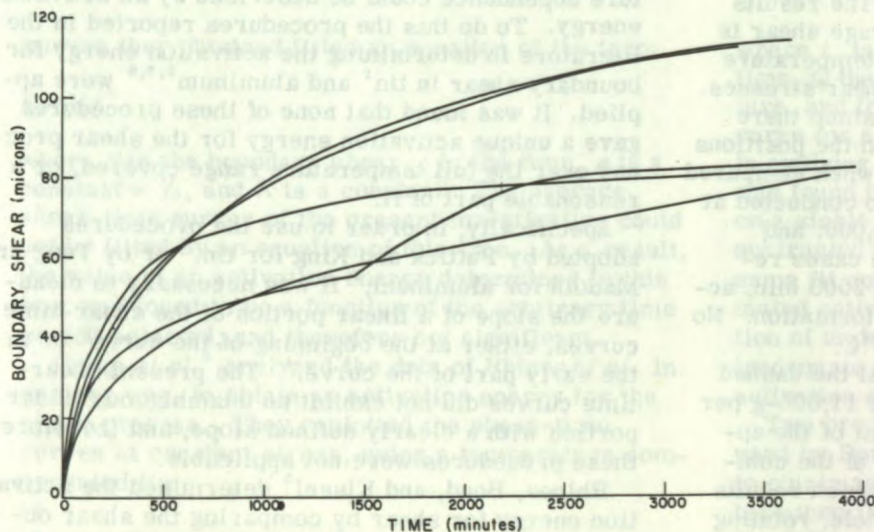


Fig. 6—Boundary shear-time curves for similar specimens tested under the same conditions. Temperature 450°C, shear stress 600 g per sq cm, orientation as in Fig. 1(c).

portion in the early part of the curve as found for tin bicrystals by Puttick and King.<sup>1</sup> There was some evidence of long-range cycling, as seen in one of the curves, which was reported by Rhines *et al.*,<sup>3</sup> but no clear evidence of the short-period cycling behavior reported by Chang and Grant<sup>6</sup> for boundaries in polycrystalline aluminum. The magnitude of the instantaneous shear observed depended on the test conditions, being most pronounced at the higher temperatures. The incubation period between application of the load and the onset of shear measured by Tung and Maddin<sup>2</sup> was not observed except in a few isolated cases.

A number of tests were conducted in which the direction of the applied shear stress was reversed after a given amount of shear had taken place, and the specimen sheared back to its original position. An example is shown in Fig. 7, in which the total shear that took place for each cycle is plotted. Curve 1 is the normal shear-time curve up to the arrow where the direction of the stress was quickly reversed. When the initial boundary position was reached, corresponding to the end of the curve, the test was stopped and the specimen was annealed at test temperature overnight. The same procedure was then repeated, resulting in curves 2 and 3. The initial boundary position was not reached on the final cycle.

From the curves in Fig. 7 it is clear that boundary shear is accompanied by work hardening and that the work hardening is not recoverable on annealing at the test temperature of 600°C. The same specimen therefore cannot be used under different test conditions and the results compared to overcome the scatter between different specimens. Note the marked increase in the shear rate when the stress is reversed in curves 2 and 3.

The scatter in the shear-time curves in Fig. 6 clearly indicated that individual tests were not adequate to describe the shear behavior of the boundary. As a result at least three repeat tests were conducted for each set of test conditions, in which six boundaries were sheared, three of which were observed during the test, and the results averaged to give the average boundary behavior. The results are shown in Fig. 8, in which the average shear is plotted as a function of time over the temperature range 300° to 600°C for a series of shear stresses. The curves for 625°C are not shown, since there appeared to be no significant change in the positions of the average curves for these tests when compared with the 600°C tests. Tests were also conducted at 250°C at shear stresses of 12,000, 16,000, and 20,000 g per sq cm, which in all three cases resulted in a maximum shear of 10  $\mu$  in 2000 min, accompanied by extensive component deformation. No significant shear was observed at 200°C.

In Fig. 8 (300°C) it will be noted that the dashed 8000-g per sq cm curve lies above the 11,000-g per sq cm curve. This is probably a result of the appreciable increase in the deformation of the component crystals at the higher stress, which results in the bending of the specimen as a whole, rotating the boundary away from the direction of the applied shear stress.

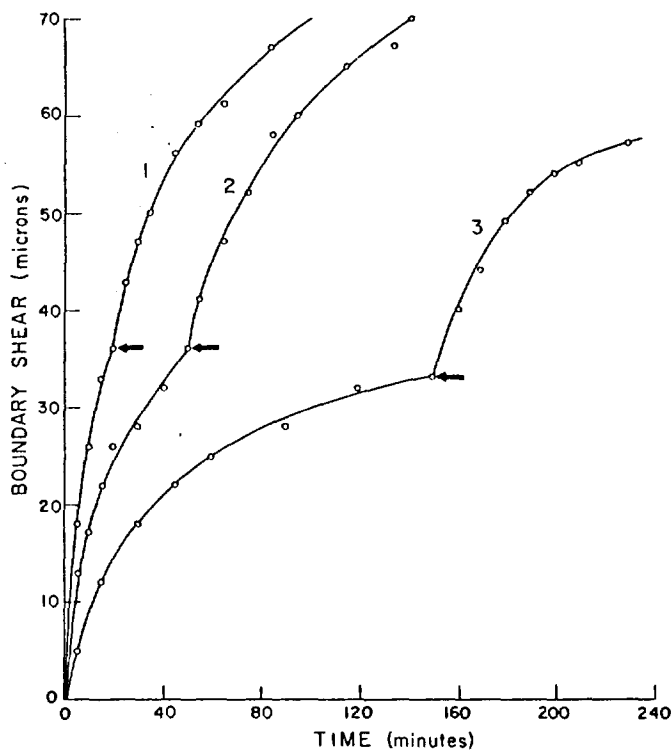


Fig. 7—Shear-time curves for a specimen in which the direction of the shear stress was reversed at the arrows. The total shear is plotted in each cycle. Temperature 600°C, shear stress 500 g per sq cm, orientation as in Fig. 1(c).

The curves shown in Fig. 8 (600° to 400°C), and the solid curves in Fig. 8 (350° and 300°C) all pertain to specimens having the orientation configuration shown in Fig. 1(c). The dashed curves in Fig. 8 (350° and 300°C) are for specimens having the orientation shown in Fig. 1(d) with  $\theta = 55$  deg. A number of tests were conducted in the 400° to 600°C region, using the 1(d) orientation ( $\theta = 55$  deg), and the resultant curves were found to coincide with those determined for the 1(c) orientation.

The average boundary shear-time curves of Fig. 8 were examined to determine whether their temperature dependence could be described by an activation energy. To do this the procedures reported in the literature in determining the activation energy for boundary shear in tin<sup>1</sup> and aluminum<sup>2,3,5</sup> were applied. It was found that none of these procedures gave a unique activation energy for the shear process over the full temperature range covered, or a reasonable part of it.

Specifically, in order to use the procedures adopted by Puttick and King for tin,<sup>1</sup> or by Tung and Maddin for aluminum,<sup>2</sup> it was necessary to measure the slope of a linear portion of the shear-time curves, either at the beginning of the curve<sup>2</sup> or in the early part of the curve.<sup>1</sup> The present shear-time curves did not exhibit an unambiguous linear portion with a clearly defined slope, and therefore these procedures were not applicable.

Rhines, Bond, and Kissel<sup>3</sup> determined the activation energy for shear by comparing the shear obtained at selected time periods, as a function of temperature, at constant stress. The shear-time

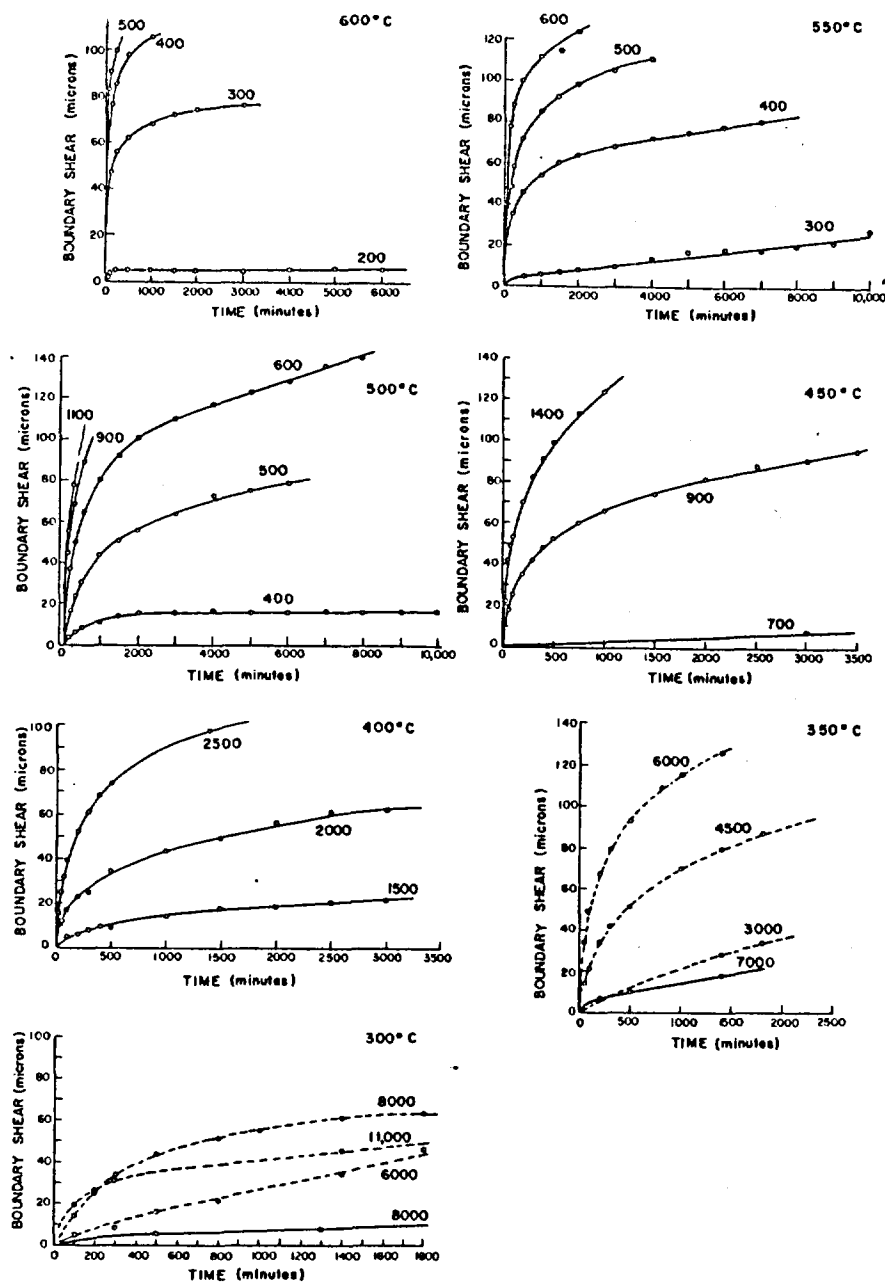


Fig. 8—Average boundary shear-time curves. Temperature and shear stress (g per sq cm) as indicated. Orientation as in Fig. 1(c) for solid lines. Orientation as in Fig. 1(d)  $\theta = 55$  deg for dashed lines.

curves they obtained fitted an equation of the form

$$S = K t^n$$

where  $S$  is the boundary shear,  $t$  is the time,  $n$  is a constant  $= 1/3$ , and  $K$  is a constant. The average shear-time curves of the present investigation could not be fitted by an equation of this type. As a result, the value of an activation energy determined in this way was found to be a function of the arbitrary time period selected, and therefore not significant.

Fazan *et al.*<sup>5</sup> analyzed the data of Rhines *et al.* in another way, to obtain an activation energy for the shear process. They replotted the shear-time curves at constant stress, using a temperature compensated time

$$t_c = t e^{-\frac{Q}{Rt}}$$

where  $t_c$  is the compensated time,  $t$  the observed time,  $Q$  the activation energy, and  $T$  the temperature, and found that all the points fell on a single curve for a correctly estimated activation energy. In applying this procedure to the present data, it was found that similar points fell reasonably well on a single curve only if an instantaneous shear was subtracted from the measured shear. Since the same fit could be obtained for a wide range of estimated activation energies by the appropriate selection of an instantaneous shear, this procedure was inadequate in the present case to determine a unique activation energy.

Two procedures were considered, which have been used by Dorn *et al.*, with polycrystalline aluminum, to obtain an activation energy for creep. They determined the time required to reach a given strain for different test temperatures, from which the activation energy was calculated.<sup>6</sup> For this procedure

to be significant, the activation energy would have to be independent of the selected strain; this was not the case when applied to the present data. The second procedure described by Dorn *et al.*<sup>9</sup> was to perform creep tests during which the test temperature was cycled periodically over a small temperature interval. The activation energy could be calculated on the basis of the change in slope of the shear-time curve, resulting from the change in temperature. Tests were conducted in this fashion, using the present tricrystal specimens, for temperature intervals of 590° to 600°C and 470° to 500°C. It was found that the measurements were not sufficiently accurate, in the case of the small displacements measured for boundary shear, to measure adequately the change in the slope of the curves with the change in temperature. There was, also, ambiguity in extrapolating the curves to the point at which the temperature was changed (about 10 min was required for the furnace to reach equilibrium). As a result this method did not give an unambiguous activation energy for the shear process.

In order to illustrate the change in behavior of the boundary shear as a function of stress and temperature—the so-called “strength” of the boundary—the stress required to produce a given shear in a given time was plotted as a function of temperature. The shear stress was estimated from the curves in Fig. 8, for shears of 10, 70, and 100  $\mu$  in 1000 min. The results are shown in Fig. 9.

It can be seen that a relatively small increase in stress is required to produce the selected shears as the temperature drops from 625° to 450°C. Below 450°C the stress increases rapidly. The curves stop when the required shear could not be obtained, as a result of rapid and extensive deformation of the component crystals.

The curves shown in Fig. 9(a) refer to specimens having the orientation configuration shown in Fig. 1(c). Similar curves for orientation 1(d)  $\theta = 55$  deg are shown in Fig. 9(b). Both orientations behave in a similar manner above 400°C.

**Boundary Angle**—For this series of tests specimens of the type shown in Fig. 1(b) were used having the orientation configuration shown in Fig. 1(d). The boundaries were of the tile type produced by rotating the center crystal about a common  $\langle 110 \rangle$  direction through an angle  $\theta$ . The boundary angle was determined from back-reflection X-ray photographs and was only correct to within about 2 deg, due to the presence of a lineage structure. Shear-time curves were obtained for a series of boundary angles and the average behavior was determined, using at least three separate tests for each curve. The results are shown in Fig. 10.

It was observed that small-angle boundaries (less than 5 deg) do not shear. This was investigated more extensively in the 500° and 600°C temperature range for a range of stresses using tilt boundaries formed by rotations about a common  $\langle 110 \rangle$  direction,  $\langle 100 \rangle$  direction, and several nonsymmetric boundaries. About thirty tests were conducted, and in all cases there was no indication that boundary shear had taken place for boundary angles less than 5 deg.

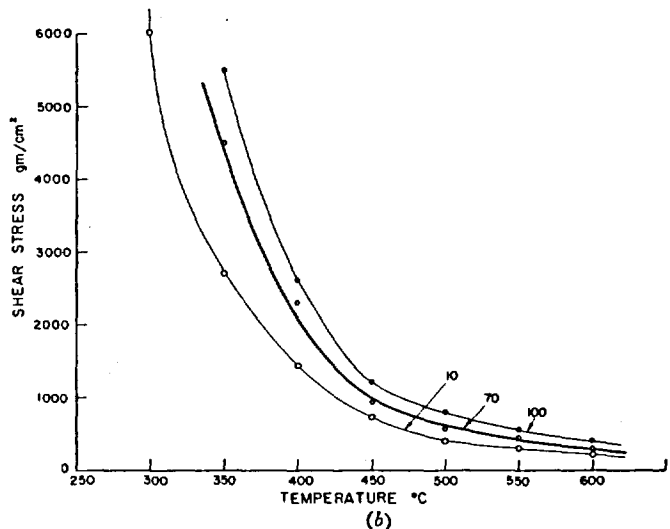
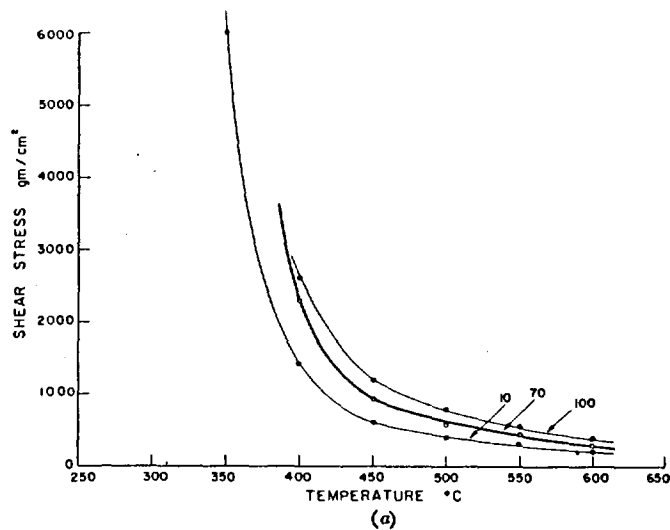


Fig. 9—Shear stress required to produce 10, 70, and 100  $\mu$  shear respectively in 1000 min as a function of temperature. (a) Orientation as in Fig. 1(c). (b) Orientation as in Fig. 1(d)  $\theta = 55$  deg.

Boundaries having tilt angles greater than 5 deg do shear, as shown in Fig. 10, the amount of shear increasing with increasing angle until an angle of about 17 deg is reached. Between 17 and 30 deg the shear is relatively independent of the boundary angle. A number of tests were conducted to determine whether other than tilt boundaries behaved in the above manner. Specimens of orientation Fig. 1(c), having a nontilt boundary of 45 deg, were tested under the same conditions; the resultant average curve was a little above the 30-deg curve shown in Fig. 10. A twist type boundary of 10 deg, produced by rotating the center crystal about an axis perpendicular to the boundary plane, resulted in an average curve a little below the 11-deg curve for the tilt boundary. It therefore appears that the boundary shear does not depend on the configuration of the component crystals, but only on the magnitude of the boundary angle under these test conditions.

It was pointed out earlier, however, that at lower temperatures there is a marked difference in the behavior of large-angle boundaries with different

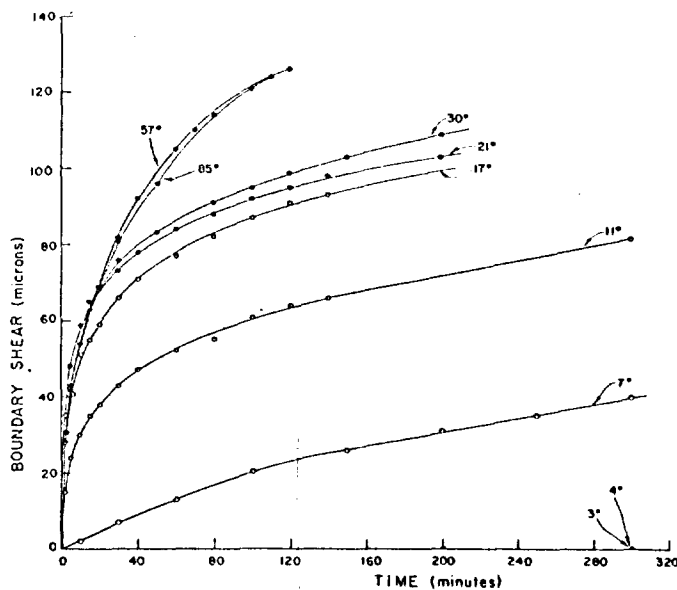


Fig. 10—Average boundary shear-time curves for the boundary angles indicated. Temperature 600°C, shear stress 500 g per sq cm, orientation as in Fig. 1(d).

configurations of component crystals. For example, at 300°C specimens of orientation Fig. 1(c) did not shear, whereas those of orientation 1(d) with  $\theta = 55$  deg did shear for the same shear stress.

The average curves for the two largest angle tests,  $\theta = 57$  deg and  $\theta = 85$  deg are seen in Fig. 10 to be superimposed and above the curve for  $\theta = 30$  deg. The results of the individual tests for both large angles had very little scatter and were all above the highest individual curve for  $\theta = 30$  deg. Consequently, the difference between the  $\theta = 57$ - and 30-deg curves is believed to be significant.

**Impurities**—The effect on the shear behavior of small additions of Cu, Fe, and Si to the super-pure aluminum was investigated. These particular elements were selected because they were the principal impurities present in the pure material, and it was considered important to ascertain whether small fluctuations in the impurity level would appreciably change the shear behavior. The amount of impurity which could be added was limited by the increasing difficulty in producing tricrystal specimens.

Parts of the tricrystals containing the impurity were chemically analyzed to determine the impurity content, and the remainder was used for test specimens. Tests were conducted at 600°C with a shear stress of 500 g per sq cm.

Additions of 0.06, 0.16, and 0.23 wt pct of Cu, 0.10 pct of Si, and 0.03 pct of Fe did not have any noticeable effect on the boundary shear behavior. These amounts are all within the solubility limits of the materials at the testing temperature. On the other hand 0.08 pct of Fe, which is not soluble in aluminum, completely inhibited shear from taking place. There was considerable difficulty experienced in growing tricrystals of this material, and it was noted that the boundaries were very irregular. As a result it is not clear whether the lack of boundary shear in this case is a result of impurities at the boundary or the increased boundary irregularity along with hardening of the component crystals. In

any event, it does not appear that small fluctuations in the impurity concentrations of the pure material should affect the observed shear behavior.

## DISCUSSION

It was observed that grain boundary shear is always accompanied by local deformation and boundary migration, providing the test was continued for a sufficiently long period of time. This suggests that the observed shear results from a number of mechanisms, each of which might be a controlling or contributing factor in the overall boundary behavior. It is likely that this is equally true in the early part of a test since shortly after the stress is applied, the rate of boundary shear decreases, the boundary trace thickens, and fine lines appear. As a result the data presented cannot be considered as representative of the behavior of a simple grain boundary.

Neighboring grains can be displaced relative to one another, under suitable test conditions, by shear along their common grain boundary at stresses less than that required to produce significant slip in the grains. This applies, as well, to the case in which the slip planes are parallel to the boundary plane and subject to the same shear stress as the boundary. This shear behavior might be accounted for in either of two ways. The presence of the boundary could result in normal slip and bending taking place near the boundary, at stresses less than that required to produce overall deformation of the grains. Or, on the other hand, shear might take place along the boundary as a result of the relatively disordered atomic structure at the boundary.

The present results tend to indicate that the second alternative might be the more reasonable. If normal slip, followed by bending, took place near the boundary, it would be expected that the deformed region should be comparable in width to the amount of shear along the boundary. This was not the case since it was observed that the width of the deformed region could be as small as  $\frac{1}{100}$  of the measured shear.

It is then postulated, following the second alternative above, that application of a shear stress along a grain boundary in the present experiments results in stress relaxation across the boundary producing shear. This would immediately result in stress concentrations at the boundary undulations followed by deformation as the shear continued.

The local deformation and boundary migration observed in the present tests are believed to result from the microscopic undulations of the boundary plane. It was observed that a large undulation could completely prevent shear from taking place, although no general correlation was found between variations in the appearance of the boundary trace and variations in shear behavior, as long as the undulations were small.

Assuming that the early deformation at the undulations consisted of crystallographic slip, then the extent and distribution of the slip lines would depend upon the size and position of the boundary undulations. This could then account for the families of



fine lines shown in Fig. 3, assuming that these lines do indicate slip lines. The deformation could also result in progressive work hardening of the material adjacent to the boundary, which in turn could account for the observation that the shear rate decreased with time after the stress was applied. It was shown in the tests in which the direction of stress was reversed, Fig. 7, that some of the work hardening could not be recovered on annealing at test temperatures.

As a boundary shear test continued, local strains associated with the work hardening in the material adjacent to the grain boundary would increase. A point would be reached where there was sufficient local strain to cause the boundary to migrate, starting at points along the boundary where the local strain was greatest, and continuing until the boundary had swept through the strained material. Shear would then commence at the new boundary position. This would then account for the alternate shear and boundary migration shown in Fig. 3.

It was observed that small angle boundaries (less than 5 deg) do not shear, and that the intermediate angles up to 17 deg sheared an increasing amount as the boundary angle increased. This would conform with the assumption that the shear process was related to boundary structure. Small angle boundaries can be described in terms of dislocation arrays where the bonding between atoms is relatively strong; large angle boundaries are considered to have relatively weak bonding between atoms. If the bonding strength of atoms in the boundary defines the ability of the boundary to shear, then the strongly bonded small angle boundaries would not shear, the large angle boundaries would shear readily, and the intermediate angles would shear an amount between these two limits depending upon the boundary angle. This would agree with the present experimental results except for the increase in shear at boundary angles of 57 and 85 deg. The latter suggests that there might be some change in the bonding of the atoms and therefore the boundary structure, as the boundary angle is increased to these large values.

The difference in behavior between the large angle boundaries of Fig. 1(c) and Fig. 1(d) ( $\theta = 55$  deg) at low temperatures might similarly be a result of boundary structure. On the other hand it could be accounted for on the basis of the local deformation accompanying shear. At high temperatures both the  $\{111\}$  and  $\{100\}$  slip systems are operative.<sup>10</sup> With the multiplicity of slip systems present it would be expected that the plastic deformation in the boundary region would be relatively insensitive to the

orientation of the component crystals, with respect to the stress axis. Below 450°C, where the difference in behavior becomes apparent, only the  $\{111\}$  slip system is operative, and therefore the orientation of the component crystals might become significant. This could result in more deformation in the Fig. 1(d) case and therefore more apparent shear.

## SUMMARY

- 1) Grain boundary shear can take place in aluminum with no apparent overall deformation of the component crystals.
- 2) Alternate boundary shear and boundary migration occur during shear accompanied by local deformation in the boundary region.
- 3) The extent of the average boundary shear is reported as a function of time, shear stress, temperature, and boundary angle.
- 4) Shear along large angle grain boundaries is a function of the orientation of the component crystals at test temperatures below 400°C.
- 5) The shear stress required to produce a given amount of boundary shear in a given time increases rapidly as the test temperature drops below approximately 425°C.
- 6) A unique activation energy could not be found which adequately described the observed temperature dependence of boundary shear.
- 7) Small variations in the impurity concentrations of copper, iron, and silicon in aluminum do not affect the boundary shear behavior.

## ACKNOWLEDGMENT

The author would like to thank Dr. E. Teghtsoonian for many helpful suggestions and discussions during the course of this investigation.

## REFERENCES

- <sup>1</sup>K. E. Puttick and R. King: Boundary Slip in Bicrystals of Tin, *Journal, Institute of Metals*, 1951-2, vol. 80, p. 537.
- <sup>2</sup>S. K. Tung and R. Maddin: Shear along Grain Boundaries in Aluminum Bicrystals, *JOURNAL OF METALS*, 1957, vol. 9, p. 905.
- <sup>3</sup>F. N. Rhines, W. E. Bond, and M. A. Kissel: Grain-Boundary Creep in Aluminum Bicrystals, *ASM Trans.*, 1956, vol. 48, p. 919.
- <sup>4</sup>D. McLean, Grain-Boundary Slip during Creep of Aluminum, *Journal, Institute of Metals*, 1952-3, vol. 81, p. 293.
- <sup>5</sup>I. Fazan, O. D. Sherby, and J. E. Dorn: Some Observations on Grain-Boundary Shearing during Creep, *JOURNAL OF METALS*, 1954, vol. 6, p. 919.
- <sup>6</sup>I. C. Chang and N. J. Grant: Observations of Creep of the Grain Boundary in High-Purity Aluminum, *JOURNAL OF METALS*, 1952, vol. 4, p. 619.
- <sup>7</sup>F. Weinberg, Grain-Boundary Shear in Aluminum, *Acta Met.*, 1954, vol. 2, p. 889.
- <sup>8</sup>B. Chalmers: The Preparation of Single Crystals and Bicrystals by the Controlled Solidification of Molten Metals, *Canadian Journal of Physics*, 1953, vol. 31, p. 136.
- <sup>9</sup>I. I-Lieh Huang, O. D. Sherby, and J. E. Dorn, Activation Energy for High-Temperature Creep of High-Purity Aluminum, *JOURNAL OF METALS*, 1956, p. 1385.
- <sup>10</sup>E. Schmid and W. Boas: *Plasticity of Crystals*, p. 85, F. A. Hughes Co., 1950.

THE QUEEN'S PRINTER AND CONTROLLER OF STATIONERY  
OTTAWA, 1959